MCB
Journals.ASM.org

Screening with a Novel Cell-Based Assay for TAZ Activators Identifies a Compound That Enhances Myogenesis in C2C12 Cells and Facilitates Muscle Repair in a Muscle Injury Model

Zeyu Yang,[a,b] Kentaro Nakagawa,[a] Aradhan Sarkar,[a] Junichi Maruyama,[a] Hiroaki Iwasa,[a] Yijun Bao,[a,c] Mari Ishigami-Yuasa,[d] Shigeru Ito,[e] Hiroyuki Kagechika,[d,e] Shoji Hata,[f] Hiroshi Nishina,[f] Shinya Abe,[g] Masanobu Kitagawa,[g] Yutaka Hata[a,h]

Department of Medical Biochemistry, Graduate School of Medical and Dental Sciences, Tokyo Medical and Dental University, Tokyo, Japan[a]; Department of Ultrasound, Shengjing Hospital of China Medical University, Shenyang, China[b]; Department of Neurosurgery, First Hospital of China Medical University, Shenyang, China[c]; Chemical Biology Screening Center[d] and Institute of Biomaterials and Bioengineering,[e] Tokyo Medical and Dental University, Tokyo, Japan; Department of Developmental and Regenerative Biology, Medical Research Institute, Tokyo Medical and Dental University, Tokyo, Japan[f]; Department of Comprehensive Pathology, Graduate School of Medical and Dental Sciences, Tokyo Medical and Dental University, Tokyo, Japan[g]; Center for Brain Integration Research, Tokyo Medical and Dental University, Tokyo, Japan[h]

The transcriptional coactivator with a PDZ-binding motif (TAZ) cooperates with various transcriptional factors and plays various roles. Immortalized human mammalian epithelial MCF10A cells form spheres when TAZ is overexpressed and activated. We developed a cell-based assay using sphere formation by TAZ-expressing MCF10A cells as a readout to screen 18,458 chemical compounds for TAZ activators. Fifty compounds were obtained, and 47 were confirmed to activate the TAZ-dependent TEAD-responsive reporter activity in HEK293 cells. We used the derived subset of compounds as a TAZ activator candidate minilibrary and searched for compounds that promote myogenesis in mouse C2C12 myoblast cells. In this study, we focused on one compound, IBS008738. IBS008738 stabilizes TAZ, increases the unphosphorylated TAZ level, enhances the association of MyoD with the myogenin promoter, upregulates MyoD-dependent gene transcription, and competes with myostatin in C2C12 cells. TAZ knockdown verifies that the effect of IBS008738 depends on endogenous TAZ in C2C12 cells. IBS008738 facilitates muscle repair in cardiotoxin-induced muscle injury and prevents dexamethasone-induced muscle atrophy. Thus, this cell-based assay is useful to identify TAZ activators with a variety of cellular outputs. Our findings also support the idea that TAZ is a potential therapeutic target for muscle atrophy.

The transcriptional coactivator with a PDZ-binding motif (TAZ, also called WWTR1) was identified as a 14-3-3-binding protein (1–3). It is similar to Yes-associated protein 1 (YAP1) in its molecular structure, which consists of an N-terminal TEAD-binding domain, one or two WW domains, and a transcriptional activation domain (4). The Hippo pathway is a tumor suppressor signaling pathway that was initially identified in *Drosophila* (2, 5, 6). TAZ is phosphorylated at four sites by large tumor suppressor kinase 1 (LATS1) and LATS2, which are core kinases of the Hippo pathway (1–3). Phosphorylated TAZ is trapped by 14-3-3, is recruited from the nucleus to the cytoplasm, and undergoes protein degradation (1–3). In this way, the Hippo pathway negatively regulates TAZ. In addition to the Hippo pathway, TAZ is regulated by cell junction proteins such as ZO-1, ZO-2, and angiomotin (7–10). Recent studies have revealed that TAZ is under the control of the actin cytoskeleton and the mechanical stretch (11–13). Moreover, Wnt signaling stabilizes TAZ (14–16). Conversely, cytoplasmic TAZ binds β-catenin and Dishevelled (DVL) and inhibits β-catenin nuclear localization and DVL phosphorylation to negatively regulate the Wnt pathway. This shows that TAZ plays a pivotal role in the cross talk between the Hippo pathway and the Wnt pathway.

In human cancers, the Hippo pathway is frequently compromised, resulting in TAZ hyperactivity (6). TAZ gene amplification is also detected in cancers (17–21). TAZ hyperactivity causes epithelial-mesenchymal transitions (EMT) and provides cancer cells with stemness (22–26). Hence, TAZ is considered a potential cancer therapeutic target. The transforming ability of TAZ is attributed mostly to the interaction with TEAD and Wbp2 (22, 27–29). Besides TEAD and Wbp2, TAZ interacts with numerous transcriptional factors. TAZ interacts with thyroid transcription factor 1, Pax8, and T-box transcription factor 5 and is important for lung, thyroid, heart, and limb development (30, 31). It also interacts with p300 (31). In human embryonic stem cells, TAZ interacts with SMAD2, -3, and -4 and is essential for the maintenance of self-renewal (16, 32, 33). In mesenchymal stem cells, TAZ interacts with peroxisome proliferator-activated receptor γ and Runx2 to suppress adipogenesis and promote osteogenesis (34, 35). In skeletal muscles, TAZ interacts with transcriptional factors that are implicated in myogenesis. It binds the key myogenic regulators Pax3 and MyoD (36, 37). TEAD binds to the so-called MCAT elements (muscle C, A, and T; 5′-CATTCC-3′) in muscle-specific genes such as that for myogenin (38). Although SMAD2 and -3, which are TAZ interactors, mediate the inhibitory signal of myostatin in muscle cells (39), TAZ is overall regarded as a myogenesis-promoting factor. This makes a sharp contrast with YAP1, whose activation induces muscle atrophy (40, 41).

Received 8 October 2013 **Returned for modification** 31 October 2013
Accepted 11 February 2014
Published ahead of print 18 February 2014
Address correspondence to Yutaka Hata, yuhammch@tmd.ac.jp.
Supplemental material for this article may be found at http://dx.doi.org/10.1128/MCB.01346-13.

doi:10.1128/MCB.01346-13

Sarcopenia is a skeletal muscle atrophy associated with ageing (42). Sarcopenia deprives elderly populations of the ability to live independently and will be a major health concern in industrialized countries. Appropriate exercise and nutrition are key factors in the prevention and treatment of sarcopenia. However, the development of drugs to increase skeletal muscles is also required. Satellite cells are considered skeletal muscle progenitor cells and a major source to regenerate muscle tissue in adults. Although the role of TAZ in the maintenance of muscle satellite cells remains to be clarified, considering the potential role of TAZ in myogenesis, we expected that TAZ activators are beneficial for the therapy of sarcopenia. We established a cell-based assay for TAZ activators, screened 18,458 chemical compounds, and obtained 50 TAZ activator candidates. We subsequently selected compounds that promote myogenesis in mouse C2C12 myoblast cells and finally focused on one compound that facilitates muscle repair in an injury model and prevents dexamethasone-induced muscle atrophy.

MATERIALS AND METHODS

DNA constructs and virus production. The pLenti-EF-ires-blast, pClneoFH, and pClneoHA vectors were described previously (43–45). A TAZ SA mutant, in which serine 89 is mutated to alanine, was prepared by the PCR method. pLenti-EF-FH-TAZ and TAZ SA-ires-blast were prepared by subcloning NheI/SalI fragments from pClneoFH-TAZ and pClneoFH-TAZ S89A into the pLenti-EF-ires-blast vector. The BLOCK-iT Pol II miR RNA interference (RNAi) expression vector kit (Invitrogen) was used to generate pcDNA knockdown constructs for human LATS1 and LATS2. The target sequences were a 1,074-bp site of LATS1 (AF104413.1) and a 1,598-bp site of LATS2 (AF207547.1). The annealing oligonucleotides were ligated into the pcDNA 6.2-GW/miR vector according to the manufacturer's protocol to generate pcDNA 6.2 LATS1 KD and pcDNA 6.2 LATS2 KD. A BamHI/XhoI fragment was isolated from pcDNA 6.2 LATS2 KD and ligated into the BglII/XhoI sites of pcDNA 6.2 LATS1 KD to generate pcDNA 6.2 LATS1/2 KD. PCR was performed on pBudCE with primers H1674 (5′-ATCGATGTCGAGCTAGCTTCGTGAG-3′) and H1675 (5′-ACTAGTCTCGAGACCACGTGTTCACGACACC-3′) to amplify the elongation factor (EF) promoter. The PCR product was digested with ClaI and SpeI and ligated into the same sites of pLenti4/TO/V5-DEST to replace the pCMV/VO promoter with the EF promoter and to generate pLenti4-EF/V5-DEST. The pLenti-EmGFP LATS1/2 KD vector was generated by using the ViraPower T-REx lentiviral expression system from pcDNA 6.2 LATS1/2 KD and pLenti4-EF/V5-DEST. The NheI/NotI fragment from pBudCE4.1 was ligated into the XbaI/NotI sites of pQCXIP (Clontech) to generate pQCXIP EF. The linker (H3142 [5′-GGCCGCTCGAGTTTAAACAATTGGATCC-3′] and H-3143 [5′-AATTGGATCCAATTGTTTAAACTCGAGC-3′]) was subcloned into the NotI/EcoRI sites to generate pQCXIP EF H3142/H3143. The BglII/NotI fragment from pClneo mCherry was ligated into the BglII/NotI sites of pQCXIP EF H3142/H3143 to generate pQCXIP mCherry, which was digested with BamHI/EcoRV, filled in, and religated to remove the internal ribosome entry sites and the puromycin resistance gene. The resulting vector was named pQCXI mCherry. pLenti-siRNA-GFP (Applied Biological Materials Inc.) was digested with SpeI/MluI. The isolated green fluorescent protein (GFP)-2A-puro fragment was subcloned into NheI/MluI sites of pClneo to generate pClneo GFP-2A-puro, which was subsequently digested with BglII/MluI. The isolated fragment was ligated into the BglII/MluI sites of pQCXI mCherry to generate pQCXI GFP2A-puromycin. WWTR1 mouse pRFP-RS short hairpin RNA (shRNA) (TF505533, 561750; OriGene) was purchased, and PCR was performed with primers H3163 (5′-CAATTGAATTCCCCAGTGGAAAGACGCGCA-3′) and H3164 (5′-ACGCGTCTCGAGCCTGGGGACTTTCACAC-3′) to amplify the U6 promoter and the target sequence. The PCR product was subcloned into the TAKN2 vector (BioDynamics Laboratory Inc.) and digested with MluI/NotI. The isolated fragment was ligated into the MluI/NotI sites of pQCXI GFP2A-puromycin. The vector was cotransfected with the pCL10A-1 retrovirus packaging vector into HEK293 cells to generate retrovirus for mouse TAZ knockdown. Lentivirus was generated as described previously (46).

Antibodies and reagents. The rat anti-YAP monoclonal antibody used was described previously (43). The following antibodies and reagents were obtained from commercial sources. The mouse anti-TAZ (560235), mouse anti-MyoD (554130), mouse anti-poly(ADP-ribose) polymerase (anti-PARP) (51-6639GR), mouse antifibronectin (610077), mouse anti-E-cadherin (610181), and mouse anti-N-cadherin (610921) antibodies and Matrigel were from BD Pharmingen. The rabbit antimyogenin (sc-576), rabbit anti-MyoD (sc-760), and mouse antivimentin (sc-6260) antibodies were from Santa Cruz. The mouse anti-myosin heavy chain (anti-MHC) (MF20), mouse anti-Pax7, and mouse anti-Pax3 antibodies were from the Developmental Studies Hybridoma Bank, University of Iowa. The rabbit antilaminin (L9293), mouse anti-α-tubulin (T9026), and mouse anti-FLAG M2 (F3165) antibodies; Hoechst 33342; *Naja mossambica* cardiotoxin; dexamethasone (C9759); epidermal growth factor (E9644); insulin (I5500), and 3-(4,5-dimethylthiazol-2-yl)-2,5-diphenyltetrazolium bromide (MTT) were from Sigma-Aldrich. Basic fibroblast growth factor (064-04541) and Phos-tag acrylamide were from Wako Chemicals. The mouse antimyogenin antibody (ab1835) was from Abcam. The mouse antihemagglutinin (anti-HA) antibody was from Roche. The mouse antiactin (clone 4) and mouse antipuromycin (clone 12D10) antibodies were from Millipore. The rabbit anti-TEAD4 antibody (APR38726_P050) was from Aviva. The goat anti-Pax3 antibody (GWB-3AE0a5) was from Genway Biotech Inc. The recombinant myostatin (788-G8-010) was from R&D Systems.

Cell culture and transfection. HEK293, A431, and HCT116 cells were cultured in Dulbecco's modified Eagle medium (DMEM) containing 10% fetal bovine serum (FBS) and 10 mM HEPES-NaOH at pH 7.4 under 5% CO_2 at 37°C. MCF10A cells were cultured in DMEM–F-12 supplemented with 5% horse serum (Invitrogen), 20 ng/ml epidermal growth factor, 0.5 μg/ml hydrocortisone, and 10 μg/ml insulin. DNA transfection was performed with Lipofectamine 2000 (Invitrogen). MCF10A-TAZ and MCF10A-TAZ SA cells were prepared with pLenti-EF-FH-TAZ-ires-blast and pLenti-EF-FH-TAZ SA-ires-blast lentivirus vectors with blasticidin selection. C2C12 cells were passaged in growth medium (DMEM containing 10% FBS) and differentiated in C2C12 differentiation medium containing DMEM and 2% horse serum (Invitrogen). C2C12 cells in which TAZ was stably knocked down were prepared with pQCXI-GFP-2A-sh mouse TAZ retrovirus. To stably knock down LATS1 and LATS2 in MCF10A-TAZ cells, the cells were infected with pLenti-EmGFP-LATS1/2 KD lentivirus and GFP-positive cells were collected by fluorescence-activated cell sorting.

Quantitative RT-PCR. Quantitative RT-PCR analysis was performed with SYBR green (Roche) and the ABI7500 real-time PCR system (Applied Biosystems) (44). For the primers used, see Table S1 in the supplemental material.

RNAi. Human TAZ and mouse TAZ were knocked down in MCF10A and C2C12 cells as described previously (44). The double-stranded RNAs (dsRNAs) used were human TAZ s24789 (Ambion) and mouse TAZ siRNA D-041057 (Dharmacon). Knockdown was confirmed by quantitative RT-PCR or immunoblotting.

Myofusion index. C2C12 cells were fixed and immunostained with anti-MHC antibody. Nuclei were visualized with Hoechst 33342. The fusion index was calculated as a percentage of the nuclei detected within MHC-positive multinuclear cells.

Reporter assay. The TEAD reporter assay was performed with HEK293 cells as described previously (43). C2C12 cells were plated at 1×10^5/well in 12-well plates and cultured overnight. The cells were transfected with the pGL3 Myo-184 (MyoD), 8×GT-IIC-δ51LucII (for TEAD), 9×CAGA-MLP (for SMAD), and $p(PRS\text{-}1/\text{-}4)_3$ (for Pax3) luciferase reporter vectors alone or with TAZ. These reporter vectors were from Kenji Miyazawa (Yamanashi University), Hiroshi Sasaki (Ku-

mamoto University), and Hiroki Kurihara (The University of Tokyo) (37, 47, 48). Dimethyl sulfoxide (DMSO) or 10 μM IBS008738 was added 6 h after transfection. The cells were grown to confluence, transferred to differentiation medium with DMSO or 10 μM IBS008738, and cultured for 24 h before luciferase assays were performed.

ChIP analysis. Chromatin immunoprecipitation (ChIP) experiments were based on the protocol described by Nelson et al. (49). In brief, C2C12 myoblasts were cultured to confluence and then treated with DMSO or 10 μM IBS008738 in differentiation medium for 24 h. Cells were cross-linked in 1.42% (vol/vol) formaldehyde for 15 min, and the reaction was quenched for 5 min with 125 mM glycine. Cross-linked cells were lysed in buffer (50 mM Tris-HCl [pH 7.5], 150 mM NaCl, 5 mM EDTA, 0.5% [vol/vol] Nonidet P-40, 1% [vol/vol] Triton X-100), and chromatin was sheared by 25 consecutive rounds in a sonicator bath (Bioruptor; Diagenode) at maximum output and cycles of 30 s on and 60 s off. Shearing was analyzed by agarose gel electrophoresis. Chromatin from about 2×10^6 cells was incubated for 3 h at 4°C with 2 μg of antibodies. Immunoprecipitation was done with 20 μl of protein G-Sepharose beads. Protein G-Sepharose without antibody was used as the control (mock ChIP). The immunoprecipitated DNA fragments were isolated with Chelex-100 resin and diluted 1:2.5 for quantitative PCR analysis. Input-normalized relative abundance was determined. For the sequences of the primers used, see Table S1 in the supplemental material.

Subcellular fractionation. Subcellular fractionation was performed as described previously (43).

Myostatin inhibition assay. C2C12 cells were transfected with control or TAZ dsRNA. Forty-eight hours later, the cells were plated in growth medium at 2×10^5/well in 12-well plates. When grown to confluence, the cells were transferred to differentiation medium with DMSO, 100 ng/ml myostatin, 10 μM IBS008738, or a combination of myostatin and IBS008738 and cultured for 3 days. The differentiation medium containing the reagents was changed every day.

Cell proliferation and viability assessment. Cell proliferation and viability were assessed by MTT formazan dye conversion.

Sphere formation assay and 3D Matrigel culture. MCF10A and A431 cells were plated at 300/well in 96-well Ultra Low Attachment plates (Corning) and cultured for 10 days in serum-free DMEM–F-12 (Invitrogen) containing 10 ng/ml basic fibroblast growth factor, 20 ng/ml epidermal growth factor, 5 μg/ml insulin, and 0.4% (wt/vol) bovine serum albumin. A cell aggregate with a diameter of more than 150 μm was defined as a sphere. For three-dimensional (3D) Matrigel culture, 96-well plates were precoated with 30 μl of Matrigel per well. Cells were suspended at 2.1×10^6/liter in medium containing 2% Matrigel. Cell suspension volumes of 140 μl containing 300 cells were plated into each well and cultured for 10 days with DMSO or 10 μM IBS008738.

Animals. All experimental procedures were approved by the Institutional Animal Care and Use Committee. Six-week-old female BALB/cByJ mice (Clea Japan Inc.) were used. *N. mossambica* cardiotoxin was dissolved in phosphate-buffered saline (PBS) at a final concentration of 10 μM. A 100-μl volume of cardiotoxin solution was injected with either control DMSO or 3 nmol of IBS008738 (0.3 μl of DMSO or 0.3 μl of 10 mM IBS008738 was diluted in 100 μl of PBS) into the tibialis anterior (TA) muscle of mice ($n = 6$) under anesthesia. Mice were sacrificed on days 2, 5, 7, and 14. For dexamethasone-induced muscle atrophy, dexamethasone (25 mg/kg/day) or DMSO was injected intraperitoneally from day 1 to day 7. A 100-μl volume of 30 μM IBS008738 or DMSO in PBS was injected into the TA and gastrocnemius (GM) muscles on days 9, 11, and 13. Mice were sacrificed on day 14.

Skeletal muscle histology. TA and GM muscles were fixed in 4% formalin and embedded in paraffin. Muscle sections 5 μm thick were stained with hematoxylin and eosin. For the immunostaining of Pax7, MyoD, and laminin, 10-μm frozen sections were fixed with acetone at −20°C for 10 min, incubated with primary antibodies at 4°C overnight, and then visualized with secondary antibodies. To quantify the extent of muscle regeneration, four sections of each muscle at 100-μm intervals were analyzed and the total number of centrally nucleated myofibers per visual field was determined manually. To assess muscle atrophy, muscles were sectioned at a 10-μm thickness and immunostained with anti-laminin antibody. The cross-sectional areas of myofibers were analyzed by using the ImageJ software.

Phosphate affinity SDS-PAGE. Phosphate affinity SDS-PAGE was performed with Phos-tag acrylamide (Wako Chemicals) and polyvinylidene difluoride (PVDF) membranes.

***In vivo* SUnSET technique.** *In vivo* SUnSET was used according to the previously reported protocol (50). Briefly, mice were anesthetized and intraperitoneally injected with 0.04 μmol/g puromycin in 100 μl of PBS. Thirty minutes later, GM muscles were removed and frozen in liquid N_2. Frozen tissues were homogenized in buffer containing 40 mM Tris-HCl at pH 7.5, 0.5% (wt/vol) Triton X-100, 1 mM EDTA, 5 mM EGTA, 25 mM β-glycerophosphate, 25 mM NaF, 1 mM Na_3VO_4, 10 mg/liter leupeptin, and 1 mM phenylmethylsulfonyl fluoride. Sixty-microgram samples of total proteins were analyzed by SDS-PAGE, and immunoblotting with antipuromycin antibody was performed with PVDF membranes. The membranes were stained with Coomassie brilliant blue.

Statistical analysis. Statistical analyses were performed with Student's *t* test for the comparison of two samples and analysis of variance with Dunnett's test for multiple comparisons with GraphPad Prism 5.0 (GraphPad Software).

Other procedures. Immunoprecipitation and immunofluorescence assay were performed as described previously (51).

RESULTS

Cell-based assay to screen for the chemical compounds that activate TAZ. We used immortalized human mammary epithelial MCF10A cells to screen for TAZ activators. LATS1- and LATS2-dependent phosphorylation at serine 89 is the key event in the regulation of TAZ. Neither parent MCF10A cells nor MCF10A cells expressing TAZ (MCF10A-TAZ) survive under mammosphere-forming conditions, while MCF10A cells expressing S89A mutant TAZ (MCF10A-TAZ SA) do form spheres (Fig. 1A). However, with LATS1 and LATS2 knockdown, MCF10A-TAZ cells, but not parent MCF10A cells, form spheres (Fig. 1B). The additional knockdown of TAZ abolished the effect of LATS1 and LATS2 knockdown in MCF10A-TAZ cells (Fig. 1C and D). These findings indicate that sphere formation by MCF10A-TAZ cells reflects the activity of overexpressed TAZ.

The screening of 18,458 chemical compounds yielded 50 TAZ activator candidates. We cultured MCF10A-TAZ cells under sphere-forming conditions with 18,458 chemical compounds at 10 μM for 14 days. Fifty compounds enabled MCF10A-TAZ cells to form spheres (we defined a cell aggregate with a longest diameter of >150 μm as a sphere). We next performed the TEAD reporter assay with these 50 compounds. Forty-seven compounds enhanced TAZ-dependent TEAD reporter activity (data not shown).

TAZ activators enhanced myogenesis in C2C12 cells. TAZ plays important roles in the regulation of osteogenesis, adipogenesis, and myogenesis (34, 52). Here we focused on myogenesis and applied 50 compounds to mouse C2C12 myoblast cells. C2C12 cells were cultured under growth conditions. After grown to confluence, the cells were switched to differentiation conditions and cultured for 72 h in differentiation medium containing 10 μM each compound. We evaluated myogenesis by determining the myofusion index (the number of nuclei detected in multinuclear MHC-positive cells divided by the total number of nuclei). Cells treated with 43 compounds exhibited higher myogenesis than control cells (data not shown). In this study, we focused on one

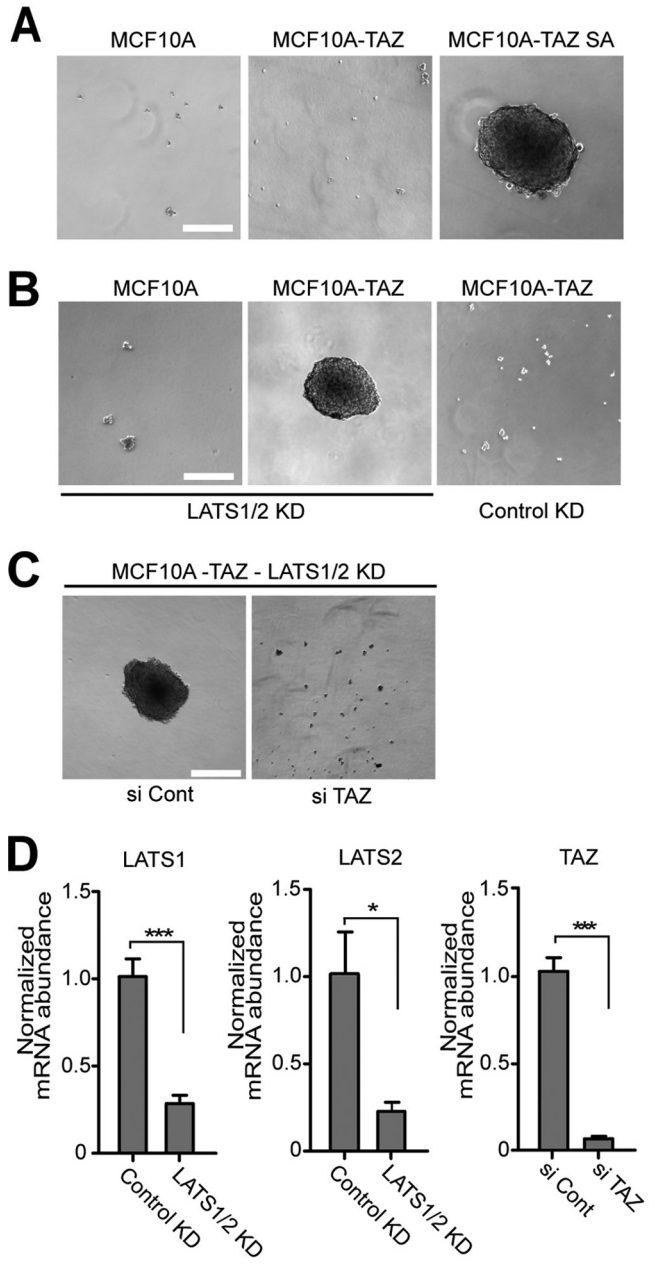

FIG 1 MCF10A cells form mammospheres depending on TAZ activity. (A) Parent MCF10A cells, TAZ-expressing MCF10A cells (MCF10A-TAZ), and TAZ SA-expressing MCF10A cells (MCF10A-TAZ SA) were cultured under mammosphere-forming conditions. Only MCF10A-TAZ SA formed spheres. (B) LATS1 and LATS2 were knocked down in parent MCF10A and MCF10A-TAZ cells. LATS1 and LATS2 knockdown (KD) provided MCF10A-TAZ cells with the capacity to form mammospheres. Parent MCF10A cells could not form mammospheres even with LATS1 and LATS2 knockdown. (C) Additional knockdown of TAZ in MCF10A-TAZ cells with LATS1 and LATS2 knockdown abolished the mammosphere formation induced by LATS1 and LATS2 knockdown. si Cont, control dsRNA; si TAZ, TAZ dsRNA. Bars, 200 μm. (D) Validation of LATS1, LATS2, and TAZ knockdowns in MCF10A cells. Data are means and standard errors of the means. *, $P < 0.05$; ***, $P < 0.001$.

compound named IBS008738, which showed the most significant effect (Fig. 2A). IBC008738 facilitated myogenesis and enhanced MHC expression (Fig. 2B). The effect was also detectable at 1 μM (Fig. 2C).

IBS008738 enhances protein expression of myogenic differentiation, and its effect depends on TAZ. When C2C12 cells were cultured with IBS008738 under growth conditions for 24 h and transferred to differentiation conditions, MyoD expression was slightly higher at 0 h (Fig. 2D). This finding suggests that IBS008738 has some ability, if not a significant one, to promote MyoD expression under growth conditions. MyoD expression more clearly increased at 24 and 48 h and declined at 72 h. Myogenin became detectable at 24 h in both control and IBS008738-treated cells, and IBS008738 increased its expression. An MHC signal started to be visible at 24 h in IBS008738-treated cells and was more apparent at 48 and 72 h than in control cells. IBS008738 also enhanced TAZ expression, with a peak at 24 h. It slightly facilitated the decrease in Pax7 but had no effect on Pax3. We knocked down endogenous TAZ with a dsRNA or shRNA retrovirus vector and confirmed that TAZ knockdown abolished the effect of IBS008738 (Fig. 2E and F).

IBS008738 enhances mRNAs of myogenic markers but not of myofusion markers. In a quantitative real-time PCR assay, the levels of transcription of the genes for myogenin and MyoD at 24 h under differentiation conditions were higher in IBS008738-treated cells but the differences were no more significant at 72 h (Fig. 3A). In contrast to TAZ protein expression, TAZ gene expression was not changed at 24 h and was reduced at 72 h. We tested the effect of IBS008738 on the expression of the genes that are regarded as TAZ targets in epithelial cells. The connective tissue growth factor (CTGF)- and cyclin D1-encoding genes were not increased in C2C12 cells by IBS008738 treatment (Fig. 3A). IBS008738 did not enhance but rather suppressed the genes for myofusion markers, including M-cadherin, calpain 1, and caveolin 3, which suggests that the enhanced myofusion observed in IBS008738-treated C2C12 cells reflects the facilitation of myogenesis at an early stage and is not directly driven by an enhanced fusion process (Fig. 3A).

IBS008738 enhances the MyoD-responsive myogenin promoter reporter in C2C12 cells. We tested whether and how IBS008738 affects the reporter activities regulated by various TAZ-interacting transcriptional factors in C2C12 cells. We exogenously expressed each reporter and TAZ in C2C12 cells and treated them with DMSO or IBS008738. TAZ overexpression enhanced the activities of all reporters, including the MyoD, TEAD, SMAD, and Pax3 reporters (Fig. 3B, first and the second columns). IBS008738 further enhanced only the MyoD reporter in C2C12 cells (Fig. 3B, second and third columns). In contrast to the result in HEK293 cells, IBS008738 did not enhance TEAD reporter activity in C2C12 cells. It did not enhance the effect of TAZ on the SMAD or Pax3 reporter either.

IBS008738 increases the association of MyoD with the myogenin promoter. MyoD, TEAD4, and Pax3 were immunoprecipitated from differentiated C2C12 cells treated with the control DMSO or IBS008738, and ChIP assays were performed. IBS008738 enhanced MyoD binding to the myogenin promoter but had no effect on the association of TEAD4 with the CTGF promoter (Fig. 3C). IBS008738 reduced the binding of Pax3 to the Myf5 promoter (Fig. 3C).

IBS008738 enhances the interaction of TAZ and MyoD. We tested the effect of IBS008738 on the interaction between TAZ and MyoD by immunoprecipitating endogenous TAZ from C2C12 cells. When MyoD was immunoprecipitated from C2C12 cells, IBS008738 slightly increased the amount of TAZ coimmunoprecipitated (Fig. 4A). However, as IBS008738 increased the expres-

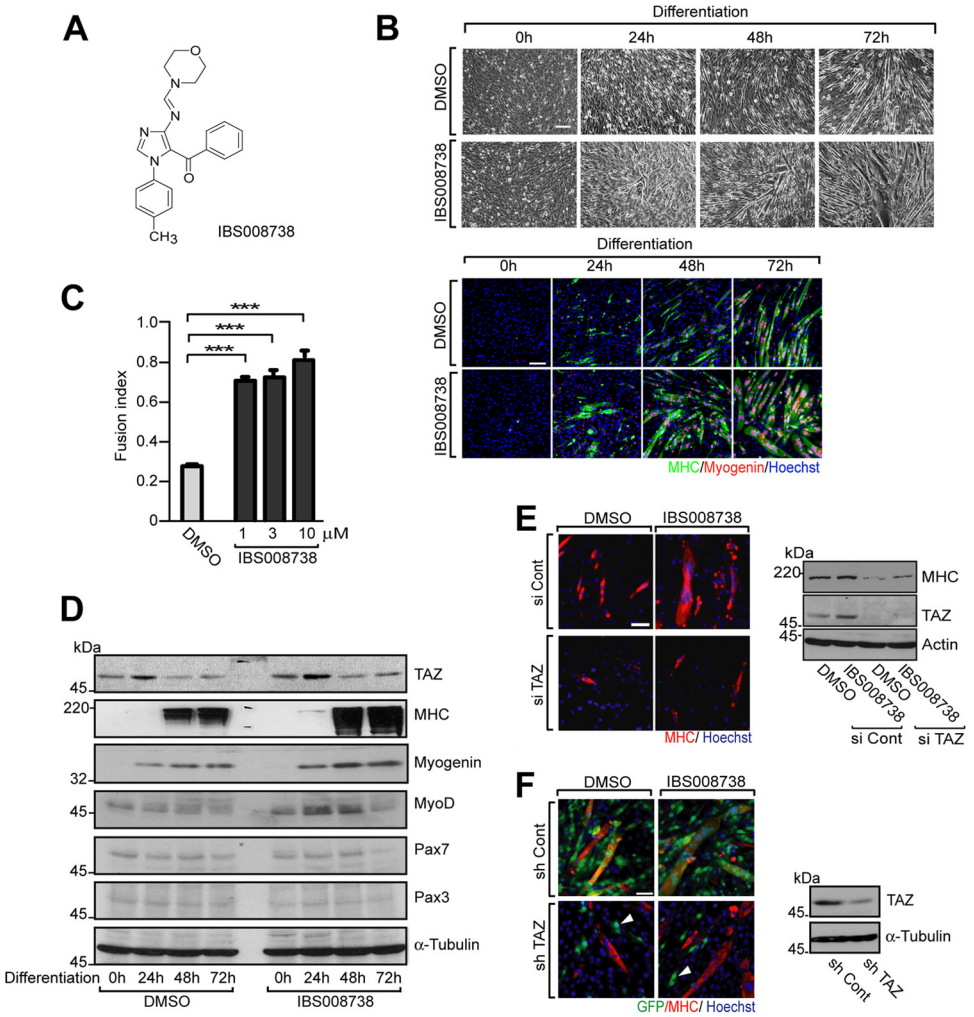

FIG 2 The TAZ activator candidate compound IBS008738 facilitates C2C12 myogenesis. (A) Chemical structure of IBS008738. (B) Phase-contrast images and immunofluorescence assays of C2C12 cells treated with DMSO or IBS008738. IBS008738 at 10 μM was added after the cells were switched to differentiation conditions. Cells were fixed at the time points indicated and immunostained with anti-MHC (green) and antimyogenin (red) antibodies (lower panels). Nuclei were visualized with Hoechst 33342. Bars, 100 μm. (C) C2C12 cells were treated with various doses of IBS008738. Myogenesis was evaluated by determining the myofusion index at 72 h. Data are means and standard errors of the means. ***, $P < 0.001$. (D) C2C12 cells were treated with DMSO or IBS008738 under growth conditions for 24 h, switched to differentiation conditions, and cultured for the indicated time periods with IBS008738 under differentiation conditions. The cells were harvested immediately after culture under growth conditions (0 h) or after 24, 48, or 72 h of culture under differentiation conditions. The lysates were immunoblotted with the antibodies indicated. α-Tubulin was used as the loading control. (E) C2C12 cells were transfected with control dsRNA (si Cont) or TAZ dsRNA (si TAZ). The cells were treated with DMSO or IBS008738 and fixed at 72 h under differentiation conditions. MHC was immunostained (red). The lysates were immunoblotted with anti-MHC and anti-TAZ antibodies. TAZ knockdown suppressed MHC expression in cells treated with DMSO (lane 3). TAZ knockdown abolished the effect of IBS008738 (lane 4). Immunoblotting with anti-TAZ antibody demonstrates that TAZ was efficiently knocked down. Bars, 100 μm. (F) Endogenous TAZ was suppressed by using shRNA in DMSO- and IBS008738-treated C2C12 cells. The retrovirus shRNA vectors harbor GFP as a tracer. MHC (red) expression is reduced in cells transfected with TAZ shRNA (green, arrowheads). The panel on the right shows the validation of shRNA.

sion of endogenous MyoD, the amount of MyoD immunoprecipitated itself increased. To circumvent this issue, we expressed FLAG-TAZ and HA-MyoD in HEK293 cells and performed immunoprecipitation with anti-FLAG M2 affinity gel. Under IBS008738 treatment, the interaction of HA-MyoD with FLAG-TAZ was enhanced (Fig. 4B, arrowhead). In the immunofluorescence of C2C12 cells, both endogenous MyoD and TAZ were diffusely distributed in the nucleus under growth conditions but formed dots under differentiation conditions (Fig. 4C, DMSO, top and middle). Interestingly, the expression of TAZ and MyoD was not the same in all of the cells. Some cells strongly expressed TAZ (red), whereas other cells expressed more MyoD (green) at 24 h after differentiation (Fig. 4C, middle). This finding is reminiscent of the previously reported heterogeneity of Myf5 expression and may suggest that MyoD and TAZ expression fluctuates like that of Myf5 in C2C12 cells (53). At 72 h in single-nucleus cells, TAZ expression decreased but MyoD was still expressed, while in multinuclear cells, both TAZ and MyoD were expressed and colocalized (yellow) in the nuclei (Fig. 4C, DMSO, bottom). IBS008738 did not have a significant effect under growth conditions. However, at 24 h under differentiation conditions, IBS008738 promoted the colocalization of TAZ and MyoD in single-nucleus cells and generated cells with two or three nuclei (Fig. 4C, IBS008738, middle, arrowheads). At 72 h, IBS008738 signifi-

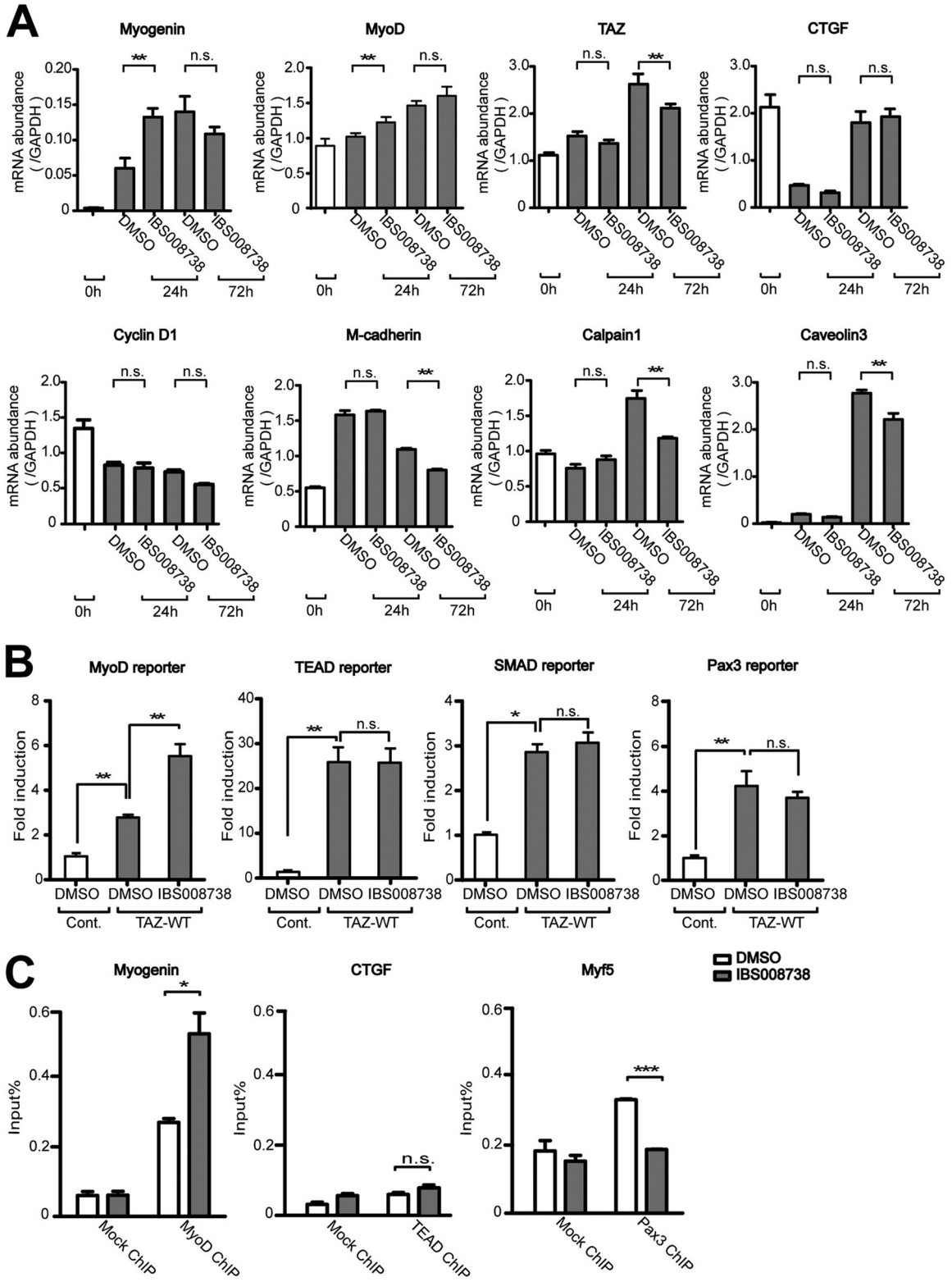

FIG 3 (A) IBS008738 enhances mRNAs of myogenic markers but not of myofusion markers. Quantitative RT-PCR was performed with mRNAs from C2C12 cells just before myogenesis induction (0 h) and from C2C12 cells treated with DMSO or IBS008738 for 24 or 72 h after myogenesis induction (24 h and 72 h). PCR was performed for myogenic markers (myogenin and MyoD), TAZ, putative targets of TAZ (CTGF and cyclin D1), and myofusion markers (M-cadherin, calpain 1, and caveolin 3). (B) IBS008738 enhances the MyoD-responsive myogenin promoter reporter in C2C12 cells. C2C12 cells were transfected with the pGL3 Myo-184-(MyoD), 8×GT-IIC-δ51LucII (for TEAD), 9×CAGA-MLP (for SMAD), and p(PRS-1/-4)3 (for Pax3) luciferase reporters alone (Cont) or with TAZ (TAZ-WT). The cells were grown to confluence and cultured for 24 h under differentiation conditions with DMSO or 10 μM IBS008738. (C) IBS008738 increases the association of MyoD with the myogenin promoter. C2C12 cells were cultured for 24 h under differentiation conditions. ChIP assay was performed with anti-MyoD (MyoD ChIP), anti-TEAD4 (TEAD ChIP), and anti-Pax3 (Pax3 ChIP) antibodies. PCR was performed to detect the promoters of myogenin, CTGF, and Myf5, respectively. Protein G-Sepharose was used as the control (Mock ChIP). In panels A to C, the data are means and standard errors of the means. *, $P < 0.05$; **, $P < 0.01$; ***, $P < 0.001$; n.s., not significant.

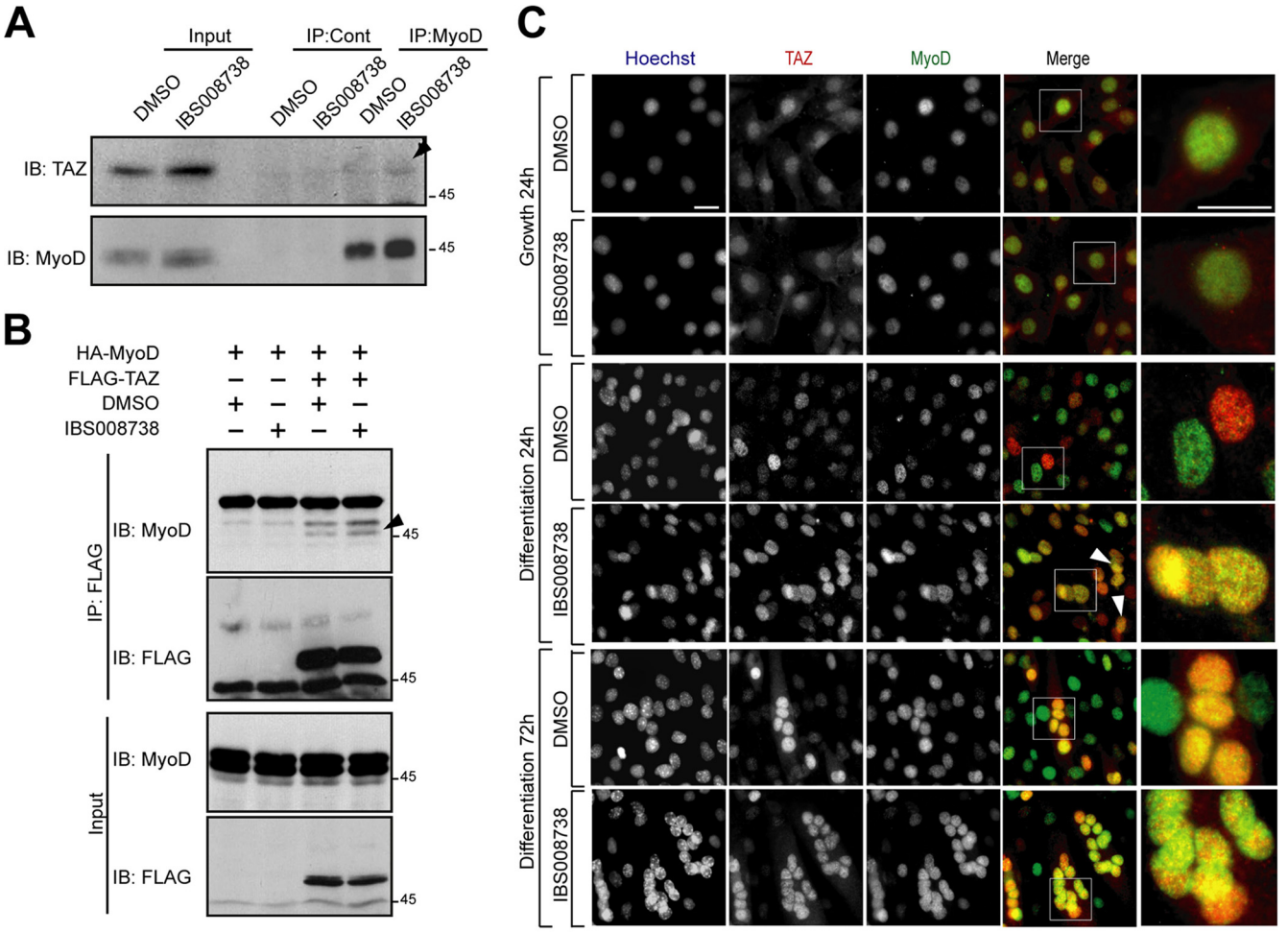

FIG 4 IBS008738 enhances the interaction between TAZ and MyoD. (A) MyoD was immunoprecipitated (IP) from DMSO- or IBS008738-treated C2C12 cells. The inputs and the precipitates were immunoblotted (IB) with anti-TAZ and anti-MyoD antibodies. TAZ immunoprecipitated from the IBS008738-treated cells increased (arrowhead). (B) HA-MyoD and FLAG-TAZ were expressed in HEK293 cells. Immunoprecipitation was performed with anti-FLAG M2 affinity gel. HA-MyoD was coimmunoprecipitated with FLAG-TAZ (third lane). IBS008738 increased the MyoD level in immunoprecipitates (arrowhead). (C) Endogenous MyoD and TAZ were immunostained in C2C12 cells at various stages. MyoD and TAZ were detected in the nuclei at all stages. Under growth conditions, both MyoD and TAZ were distributed diffusely in the nuclei. Under differentiation conditions, MyoD and TAZ formed dots in the nuclei. At 24 h after myogenesis induction, not all of the control cell nuclei expressed MyoD (green) and TAZ (red) equally. During treatment with IBS008738, the merged images are more yellowish, showing that MyoD and TAZ are better colocalized. Arrowheads indicate cells with two or three nuclei. Bar, 50 μm.

cantly increased the percentage of multinuclear cells (Fig. 4C, IBS008738, bottom).

IBS008738 increases the level of unphosphorylated TAZ in C2C12 cells. In epithelial cells, subcellular localization is important in TAZ activity regulation. However, consistent with the immunofluorescence results, in C2C12 cells, TAZ was detected mainly in the nuclear fraction and IBS008738 showed no significant effect on subcellular localization (Fig. 5A). To further characterize the effect of IBS008738 on TAZ, we analyzed TAZ by phosphate affinity SDS-PAGE. TAZ with serine 89 unphosphorylated, which was detected by anti-TAZ antibody (Fig. 5B, left) but not with antibody specific for TAZ with serine 89 phosphorylated (Fig. 5B, right), slightly increased (Fig. 5B, an arrow). However, phosphorylated TAZ also slightly increased, which means that IBS008738 increases the total amount of TAZ. Moreover, phosphorylated and unphosphorylated TAZ from IBS008738-treated cells exhibited mobility different from that of TAZ from control C2C12 cells (Fig. 5B, arrowhead). This finding suggests that in C2C12 cells, even TAZ with serine 89 unphosphorylated is localized in the nucleus and that IBS008738 induces some modification of TAZ, which is distinct from the phosphorylation at serine 89. We also tested the stability of TAZ. In control C2C12 cells, TAZ gradually decreased when protein synthesis was blocked by cycloheximide (Fig. 5C, DMSO). In IBS008738-treated C2C12 cells, TAZ expression was increased and degradation was delayed (Fig. 5C, IBS008738). IBS008738 is likely to stabilize TAZ.

Effect of IBS008738 on TAZ in MCF10A cells. As we used MCF10A cells in the original screening, we wanted to know whether IBS008738 has a similar effect on TAZ in MCF10A cells. The knockdown of TAZ in MCF10A-TAZ cells blocked sphere formation during treatment with IBS008738 (data now shown). Therefore, IBS008738-induced sphere formation indeed depends on TAZ. In the subcellular fractionation of MCF10A-TAZ cells that were cultured under sphere-forming conditions, IBS008738 increased the amount of nuclear TAZ (Fig. 5D, arrowhead). In MCF10A-TAZ cells, IBS008738 enhanced CTGF-encoding gene

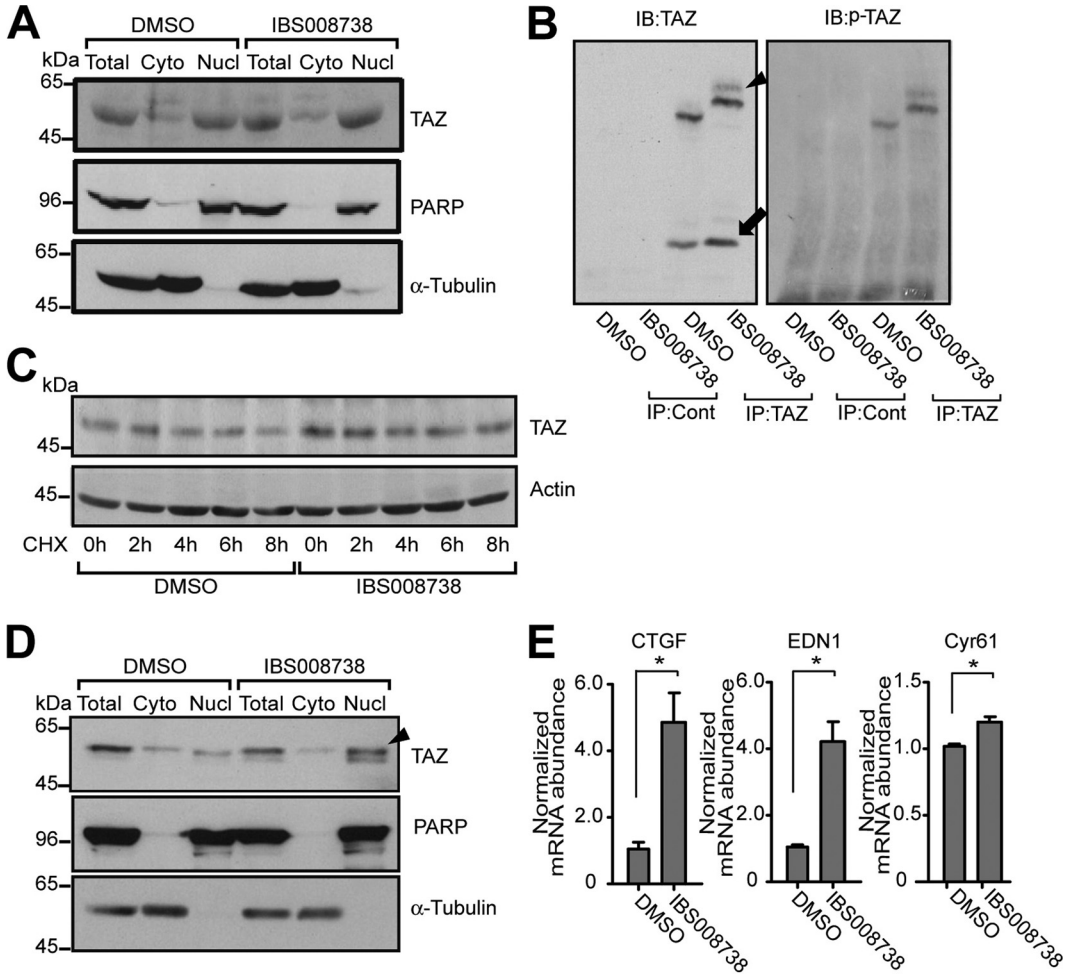

FIG 5 (A) Subcellular TAZ localization in C2C12 cells. Subcellular fractionation of C2C12 cells cultured for 24 h under differentiation conditions was performed. TAZ was recovered mainly in the nuclear fraction. IBS008738 did not significantly influence the distribution of TAZ. PARP and α-tubulin were used as nuclear and cytosolic markers, respectively. (B) TAZ was immunoprecipitated (IP) from lysates of DMSO- and IBS008738-treated C2C12 cells, analyzed by phosphate affinity SDS-PAGE, and immunoblotted with anti-TAZ antibody and anti-serine 89-phosphorylated TAZ-specific antibody, which recognizes the phosphorylation at serine 89. The lower band, which was detected by the anti-TAZ antibody but not by the anti-serine 89-phosphorylated TAZ-specific antibody, increased during treatment with IBS008738 (arrow). The upper bands, which were recognized by anti-serine 89-phosphorylated TAZ-specific antibody, exhibited a different mobility shift with IBS008738 treatment (arrowhead). (C) C2C12 cells were treated with DMSO or 10 μM IBS008738 for 24 h under differentiation conditions and then treated with 50 μg/ml cycloheximide (CHX). TAZ was immunoblotted at the time points indicated. TAZ expression gradually decreased in DMSO-treated C2C12 cells. TAZ expression increased in IBS008738-treated cells, and the decrease was delayed. (D) TAZ in the subcellular fractions of MCF10A-TAZ cells. TAZ was distributed equally in the cytoplasm and the nucleus. IBS008738 increased the nuclear TAZ level (arrowhead). (E) IBS008738 increased the levels of the mRNAs of the TAZ target genes for CTGF, EDN1, and Cyr61 in MCF10A cells. Data are means and standard errors of the means. *, $P < 0.05$.

transcription (Fig. 5E). It also enhanced EDN1 mRNA and to a lesser extent Cyr61 mRNA (Fig. 5E). These findings suggest that IBS008738 increases the nuclear TAZ level in both C2C12 and MCF10A cells but that the genes upregulated are determined in a cell context-dependent manner.

IBS008738 is most effective when applied for the first 24 h under differentiation conditions. To determine the stage at which IBS008738 influences myogenesis, we treated C2C12 cells with the compound at various time points. First, we treated C2C12 cells with various doses of IBS008738 under growth conditions, but IBS008738 had no effect on cell proliferation (Fig. 6A). Next we treated C2C12 cells for various times under differentiation conditions. Treatment during the first 24 h upregulated MHC (Fig. 6B). The expression of myogenin and MyoD was also enhanced (Fig. 6C, arrowheads). In contrast, treatment at 24 to 48 h or 48 to 72 h did not have a significant effect. These findings suggest that IBS008738 is most effective when it is applied during the initial phase of differentiation.

IBS008738 competes with myostatin. Myostatin is a member of the bone morphogenetic protein/transforming growth factor β superfamily and inhibits muscle growth and differentiation. It binds the activin type IIB receptor and triggers SMAD2- and -3-dependent signaling. As TAZ interacts with SMAD2 and -3, we wanted to know whether and how IBS008738 modulates myostatin signaling. Myostatin inhibited myogenesis in C2C12 cells, but IBS008738 restored myogenesis (Fig. 7A, si Cont). TAZ knockdown itself inhibited myogenesis and canceled the effect of IBS008738 (Fig. 7A, si TAZ). The myofusion index corroborated

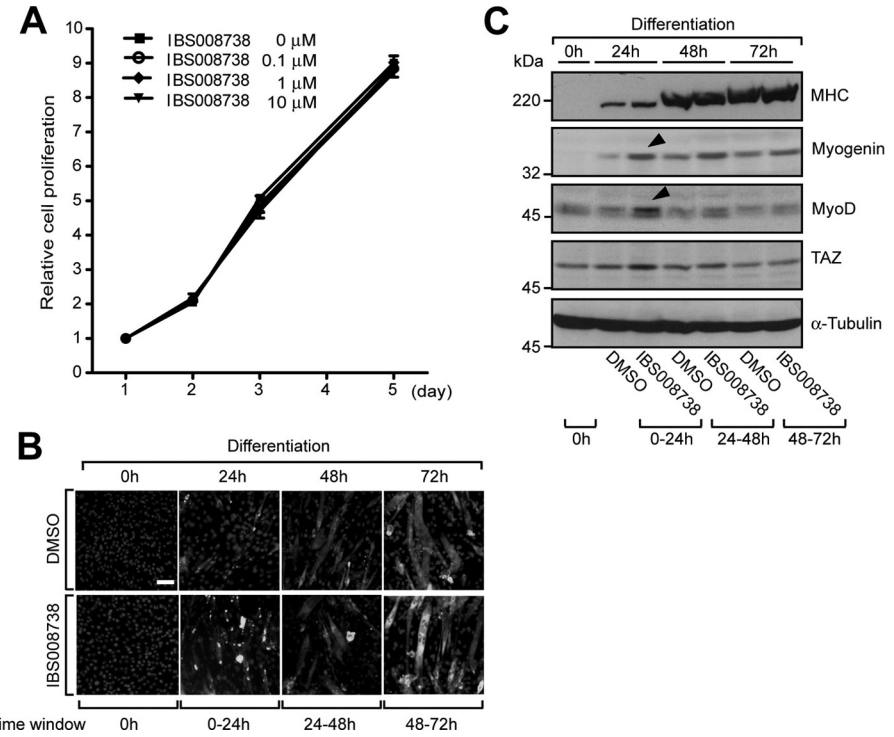

FIG 6 (A) C2C12 cells were cultured under growth conditions with various doses of IBS008738. Viable-cell numbers were evaluated by MTT assay. The value on day 1 after plating was set at 1. IBS008738 had no effect on cell proliferation. (B and C) C2C12 cells under differentiation conditions were treated with 10 μM IBS008738 during the time periods indicated (0 to 24, 24 to 48, and 48 to 72 h). Cells were harvested after treatment (at 24, 48, or 72 h). (B) Immunofluorescence images of MHC (white). Bar, 100 μm. (C) Immunoblotting of MHC, MyoD, myogenin, and TAZ. IBS008738 most significantly enhanced myogenin and MyoD when cells were treated during the first 24 h under differentiation conditions (arrowheads).

the immunofluorescence assay observation (Fig. 7B). In the immunoblotting assay, the MHC level decreased in myostatin-treated cells but IBS008738 restored it (Fig. 7C, second and third lanes). TAZ knockdown attenuated the restoration of MHC expression by IBS008738 (Fig. 7C, fifth and sixth lanes).

IBS008738 facilitates muscle repair in cardiotoxin-injected muscles. To assess the effect of IBS008738 on muscle regeneration, we injected cardiotoxin with control DMSO or IBS008738 into TA muscles. Hematoxylin-eosin staining showed that centrally nucleated fibers, a hallmark of regeneration, increased in IBS008738-injected muscles (Fig. 8A). To quantitatively evaluate muscle fiber size, we immunostained laminin, measured the sizes of myofibers demarcated by laminin, and confirmed the effect of IBS008738 (Fig. 8B). Pax7-positive cells, which were detected under the basal lamina, increased on day 5, decreased on day 7, and returned to the control level on day 14, whereas the number of MyoD-positive cells remained high on days 5 and 7 (Fig. 8C and D). All of these findings support the idea that IBS008738 facilitates muscle regeneration in response to injury.

IBS008738 prevents dexamethasone-induced muscle atrophy. We also induced muscle atrophy by dexamethasone administration in BALB/cByJ mice ($n = 6$ DMSO control, $n = 6$ dexamethasone treated) and injected IBS008738 three times into one hind limb muscle and control DMSO into the contralateral muscle. The mice were sacrificed on day 14. Dexamethasone treatment reduced muscle weights (Fig. 9A, first and third columns). IBS008738 did not increase muscle weights in control mice but prevented a dexamethasone-induced muscle decrease (Fig. 9A, second and fourth columns). Hematoxylin-eosin staining also showed a dexamethasone-induced reduction of muscle fiber size (Fig. 9B, upper panels). IBS008738 itself caused no significant change but prevented dexamethasone-induced muscle atrophy (Fig. 9B, lower panels). A quantitative evaluation of muscle fiber size confirmed the effect of IBS008738 (Fig. 9C). To measure protein synthesis, we injected puromycin 30 min before dexamethasone-treated mice were sacrificed and immunoblotted muscle lysates from the mice ($n = 3$ DMSO control, $n = 3$ IBS008738 treated) with antipuromycin antibody. IBS008738 significantly increased the incorporation of puromycin, suggesting that protein synthesis was enhanced in IBS008738-treated mice (Fig. 9D). Muscle-specific E3 ubiquitin ligases, MuRF-1, and atrogin-1 (MAFbx) are involved in glucocorticoid-induced muscle atrophy (54). Dexamethasone increased the MuRF-1 and atrogin-1 mRNA levels in GM muscles, but IBS008738 decreased them (Fig. 9E). These findings suggest that IBS008738 prevents dexamethasone-induced muscle atrophy through the inhibition of protein degradation and enhancement of protein synthesis.

IBS008738 does not significantly influence the malignant properties of cancer cells. We expect that IBS008738 is a promising lead compound for the development of a drug to prevent muscle atrophy and facilitate muscle regeneration after injury. However, TAZ is known as an oncogene and the hyperactivity of TAZ induces EMT of cancer cells. The effects of IBS008738 on the TEAD and SMAD reporters are not so significant in C2C12 cells, yet we need to consider the risk of IBS008738 application. We tested whether and how IBS008738 induces EMT in cancer cells. It

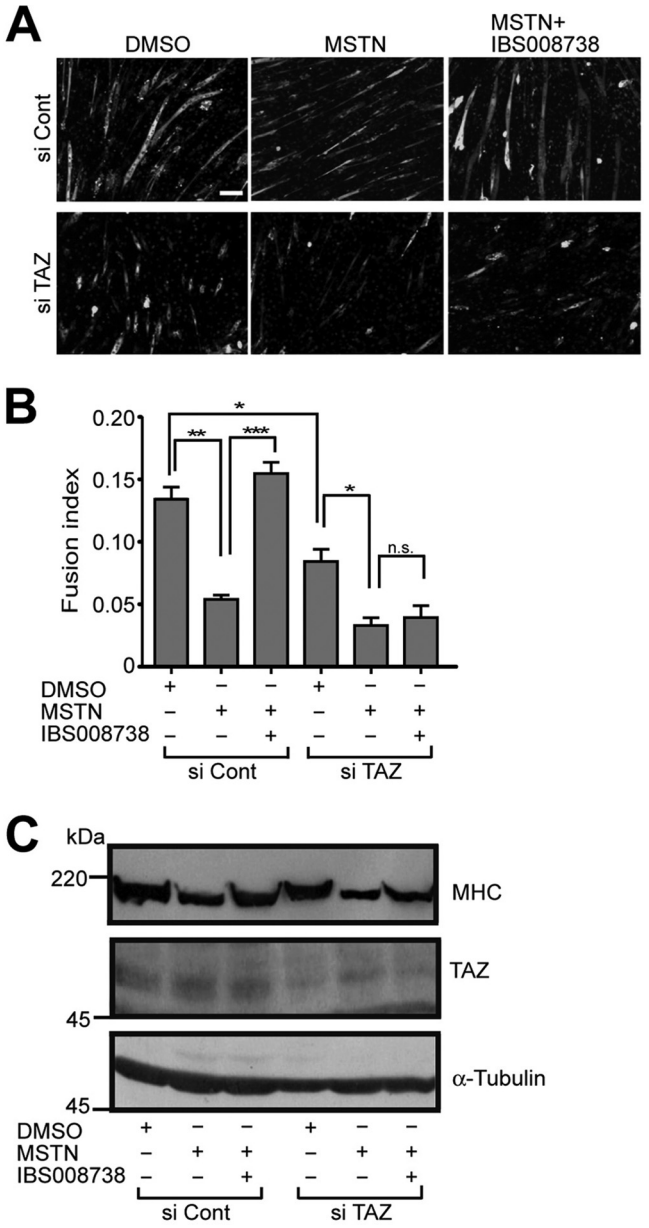

FIG 7 IBS008738 competes with myostatin. C2C12 cells were transfected with control dsRNA (si Cont) or TAZ dsRNA (si TAZ). Cells were grown to confluence and switched to differentiation conditions. Cells were cultured for 72 h with DMSO, 100 ng/ml myostatin (MSTN) alone, or 100 ng/ml myostatin with 10 μM IBS008738 as indicated. (A) Immunofluorescence images of MHC. Bar, 100 μm. (B) Myofusion index. Data are means and standard errors of the means. *, $P < 0.05$; **, $P < 0.01$; ***, $P < 0.001$; n.s., not significant. (C) Cell lysates were immunoblotted with the antibodies indicated.

did not enhance EMT marker protein expression in A431, A549, or HCT116 cells (Fig. 10A). IBS008738 did not enhance tumor sphere formation or the 3D Matrigel growth of A431 cells either (Fig. 10B).

DISCUSSION

In this study, we established a cell-based assay to search for TAZ activators. MCF10A-TAZ SA cells, which are unresponsive to negative regulation by the Hippo pathway, robustly form spheres under mammosphere-forming conditions, while parent MCF10A and MCF10A-TAZ cells lack the capacity to form spheres (Fig. 1). However, LATS1 and LATS2 knockdown makes MCF10A-TAZ cells, but not parent MCF10A cells, form spheres. The additional knockdown of TAZ in MCF10A-TAZ cells with LATS1 and LATS2 knockdown abolished sphere formation. These results indicate that MCF10A-TAZ cells acquire the capacity to form spheres when TAZ is activated. Therefore, we used this assay to identify compounds that activate TAZ. It is not clear which transcriptional factor is implicated in TAZ-dependent sphere formation by MCF10A cells. Among the TAZ-interacting transcriptional factors, TEAD proteins have been shown to be implicated in TAZ-mediated EMT (29). As EMT is related to stemness in cancer cells, genes transcribed by TEAD may be required for sphere formation. Most of the compounds obtained through this assay augment TAZ-dependent upregulation of TEAD-responsive reporter activity in HEK293 cells. The enhancement by the compounds is only 2-fold, but as cells are exposed to the compounds for a longer time in the sphere formation assay, the modest enhancement might be sufficient to induce sphere formation.

This assay gives compounds with disparate targets. The regulation of TAZ is multifaceted. The Hippo pathway, junction proteins, the actin cytoskeleton, and the Wnt pathway regulate TAZ. The compounds may upregulate TAZ through these regulatory mechanisms. Our preliminary experiments suggest that the compounds show different effects on the differentiation of mouse mesenchymal stem cells (data not shown). Some compounds strongly promote osteogenesis, while others do not. The inhibitory effects on adipogenesis are also unequal. These findings support the idea that each compound activates TAZ through a distinct mechanism. YAP1 is a paralog of TAZ. The molecular structures of YAP1 and TAZ are similar. YAP1 is regulated by the Hippo pathway, junction proteins, and the actin cytoskeleton in a manner similar to that of TAZ regulation (3, 12, 13). If the compounds work through the same regulatory mechanisms, the compounds should activate YAP1 too. Indeed, some of them enhance YAP1-dependent TEAD-responsive reporter activity, but not all of the compounds are active for YAP1. This observation also implies that the targets of 50 TAZ activator candidates are not the same. Thus, this new cell-based assay provided us with a collection of 50 TAZ activator candidate compounds that exhibit various cellular outputs and have distinct molecular targets.

As TAZ promotes osteogenesis and inhibits adipogenesis in mesenchymal stem cells, it is tempting to use TAZ activators therapeutically against osteoporosis and obesity. The osteogenic and antiadipogenic effects of kaempferol, a dietary flavonoid, depend on TAZ, supporting the notion that TAZ can be a therapeutic target in osteoporosis and obesity (55). Accordingly, the TAZ activator TM-25659 has been proposed to be beneficial in the control of osteoporosis and obesity (56). However, in the treatment of osteoporosis, the patients are females after menopause and relatively young. Once drug application starts, it is not easy to stop it. The oncogenic property of TAZ is an obstacle in the application of TAZ activators to osteoporosis. In the treatment of sarcopenia, the patients are extremely old. Once sufficient muscles are acquired for the rehabilitation program, the drug can be withdrawn. As the recovery of lower limb muscles is the most important, local application to those muscles by injection or percutaneously might be sufficient and systemic application could be avoided. Therefore, we expect that the treatment of sarcopenia with TAZ activators is

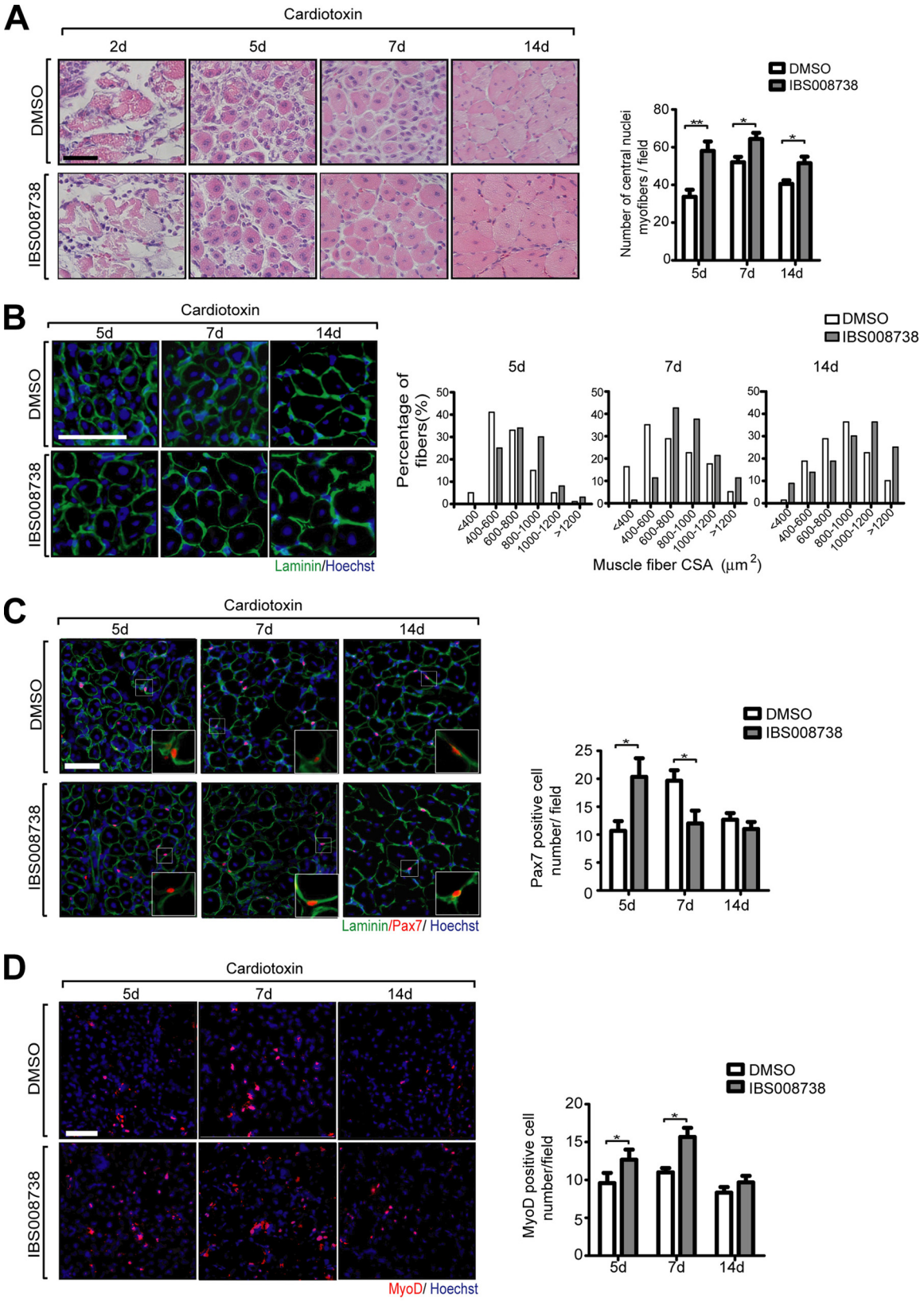

FIG 8 IBS008738 facilitates the repair of cardiotoxin-injected muscles. (A) Cardiotoxin was injected into TA muscles with control DMSO or IBS008738. The muscles were fixed at the time points indicated. The centrally nucleated fibers in nine independent fields of each muscle were counted at ×20 magnification. (B) Tissues were immunostained with antilaminin antibody. Cross-sectional areas (CSA) of myofibers were measured. Five hundred myofibers in each mouse sample were analyzed. Data from three mice are shown. (C and D) Tissues were immunostained with anti-Pax7 (red) and antilaminin (green) antibodies in panel C and with anti-MyoD antibody (red) in panel D at the time points indicated. In panel C, the marked fields are shown at higher magnification in the insets. The Pax7- and MyoD-positive cells in six independent fields of each muscle were counted at ×20 magnification. The data summarize the results obtained from three mice. In panels A, C, and D, the data are means and standard errors of the means. *, $P < 0.05$; **, $P < 0.01$. Bar, 50 μm.

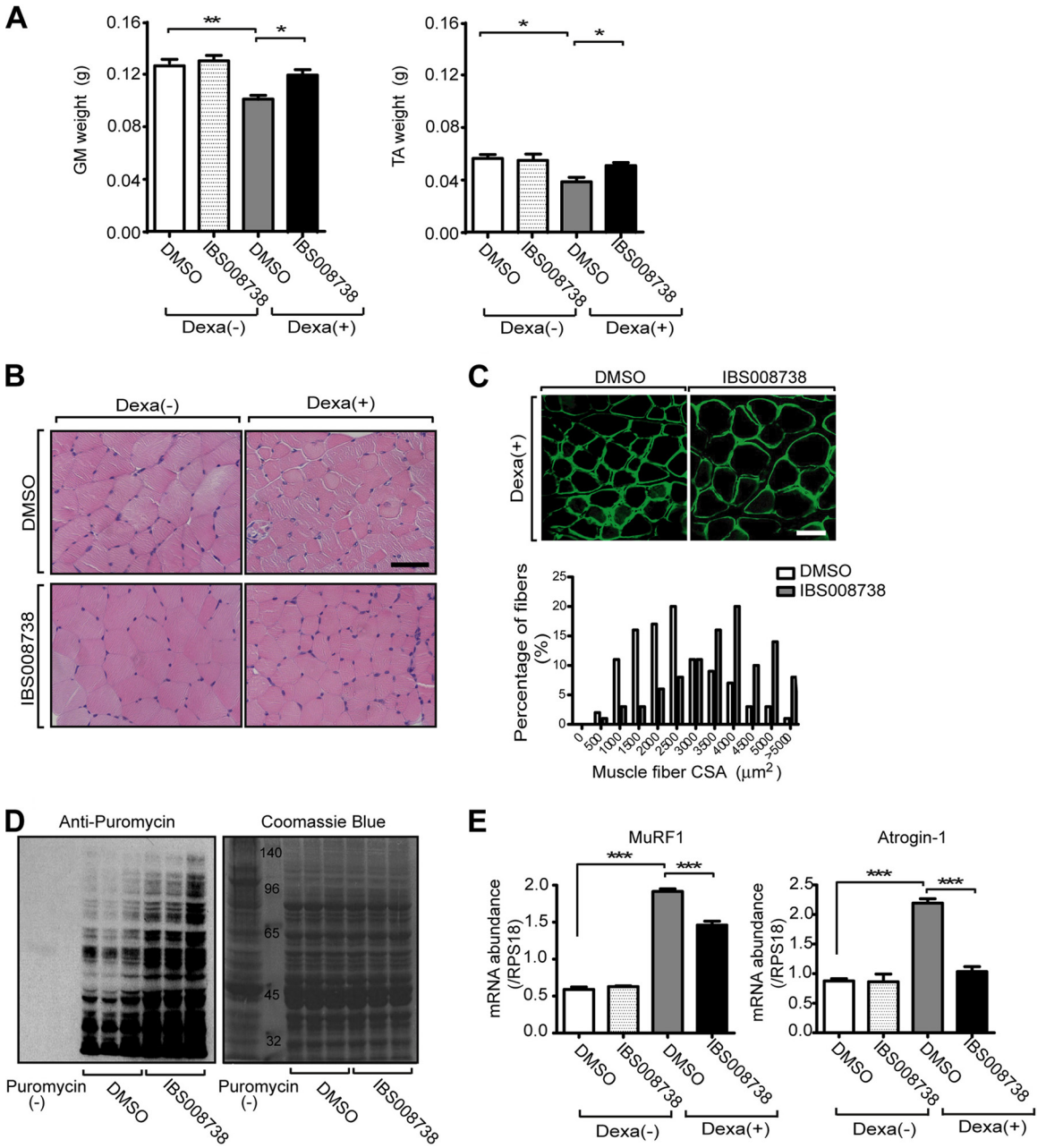

FIG 9 IBS008738 prevents dexamethasone-induced muscle atrophy. Dexamethasone (Dexa; 25 mg/kg/day) was intraperitoneally injected into 6-week-old female BALB/cByJ mice for 1 week. Control DMSO or IBS008738 was injected into their hind limbs every other day. On day 14, muscles were fixed. (A) Weights of GM and TA muscles. (B) Tissues were stained with hematoxylin and eosin. Dexamethasone induced muscle atrophy (upper panels). IBS008738 partially blocked atrophy (lower panels). Bar, 50 μm. (C) Cross-sectional areas (CSA) of myofibers were analyzed as described in the legend to Fig. 8B. (D) Puromycin was injected intraperitoneally 30 min before dexamethasone-treated mice were sacrificed. Puromycin-labeled proteins in GM muscles were detected with antipuromycin antibody (left panel). Samples of three DMSO-treated and three IBS008738-treated muscles were run side by side. A sample from a mouse with no injection of puromycin was run in the first lane. To confirm that the same amount of proteins was run in each lane, the membranes were stained with Coomassie brilliant blue (right panel). (E) Quantitative RT-PCR was performed with mRNAs from GM muscles. IBS008738 partially suppressed the dexamethasone-induced increase in the MuRF-1 and atrogin-1 mRNAs. In panels A and E, the data are means and standard errors of the means. *, $P < 0.05$; **, $P < 0.01$; ***, $P < 0.001$.

more realistic. Hence, we selected compounds that facilitate myogenesis in mouse C2C12 myoblast cells and expected that such compounds may also promote satellite cell proliferation and differentiation. In this study, we focused on one compound, IBS008738.

The effects of IBS008738 on sphere formation by MCF10A-TAZ cells and myogenesis of C2C12 cells are both abolished by TAZ knockdown. This indicates that the effect of IBS008738 depends on TAZ. In MCF10A-TAZ cells, IBS008738 increases the nuclear TAZ level (Fig. 5). In C2C12 cells, IBS008738 increases the

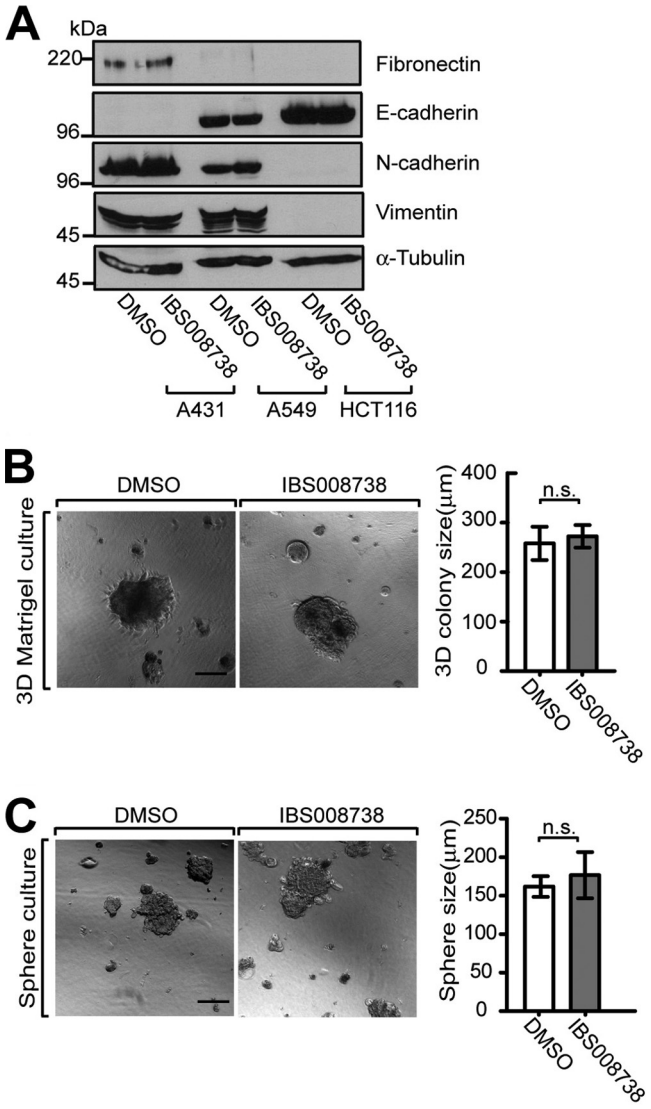

FIG 10 Effect of IBS008738 on cancer cells. (A) Human epidermal cancer A431, lung cancer A549, and colon cancer HCT116 cells were treated with IBS008738. Cell lysates were immunoblotted with the antibodies indicated. (B and C) A431 cells were cultured under sphere-forming conditions (B) or in 3D Matrigel (C). The maximum diameters of 30 cell aggregates with diameters of >150 μm were measured. IBS008738 did not enhance tumor sphere formation or the growth of A431 cells in 3D Matrigel. Bar, 200 μm. In panels B and C, the data are means and standard errors of the means. n.s., not significant.

unphosphorylated TAZ level. These changes also support the idea that IBS008738 indeed works on TAZ. Phosphate affinity SDS-PAGE analysis suggests that IBS008738 induces modifications of TAZ other than phosphorylation at serine 89. It will be intriguing and necessary to determine the molecular modifications by mass spectrometry. Phosphate affinity SDS-PAGE has additionally revealed that almost 50% of the TAZ in C2C12 cells is phosphorylated but that most of the TAZ is localized in the nucleus. This finding implies that the phosphorylated TAZ in C2C12 cells cannot be captured in the cytoplasm or is retained by the nucleus. This might be due to the limited amount of 14-3-3 or the abundance of nuclear transcriptional factors such as MyoD that interact with TAZ. The effects of IBS008738 on gene transcription are different in MCF10A and C2C12 cells. IBS008738 increases CTGF mRNA in MCF10A cells but not in C2C12 cells (Fig. 3). Likewise, IBS008738 enhances TEAD-responsive reporter activity in HEK293 cells but not in C2C12 cells. These discrepancies may reflect the different expression of TEAD and MyoD in these cells, and TAZ may select the interacting partners in a cell context-dependent manner. On the basis of our reporter and ChIP assays, we speculate that in C2C12 cells, MyoD is the main partner of TAZ under differentiation conditions and that consequently MyoD-mediated cellular outputs are most prominent in IBS008738-treated C2C12 cells.

IBS008738 enhances MyoD expression in C2C12 cells under growth conditions and accelerates myogenesis under differentiation conditions (Fig. 2). The *in vitro* interaction experiment and the immunofluorescence assay support the idea that IBS008738 augments the association of TAZ with MyoD (Fig. 4). IBS008738 stabilizes TAZ and increases its protein expression (Fig. 5). IBS008738 promotes the association of MyoD with the myogenin promoter (Fig. 3C). The binding of Pax3 to the Myf5 promoter decreased in IBS008738-treated cells. This finding is understandable, because Myf5 is known to be downregulated early in differentiation (53). As the ChIP assay was performed 24 h after differentiation, we speculated that this decrease may mirror the rapid myogenesis that occurs during IBS008738 treatment. The competition of IBS008738 with myostatin is equivocal. As SMAD2 and -3 mediate myostatin signaling and TAZ cooperates with SMAD2 and -3 in human embryonic stem cells and mouse embryos, TAZ activators are postulated to enhance myostatin signaling but IBS008738 competes with myostatin in the myogenesis of C2C12 cells (Fig. 7). We here infer again that the effect of IBS008738 on MyoD is more prominent because MyoD is more abundant than SMAD2 and -3 in C2C12 cells.

IBS008738 increases the numbers of Pax7-positive cells in the early phase and centrally nucleated fibers in injured muscles. Later, the number of Pax7-positive cells decreases while that of MyoD-positive cells increases (Fig. 8). Pax7 is thought to play dual roles in the regeneration of skeletal muscles (57). Pax7 promotes progenitors to commit to the skeletal muscle lineage but blocks terminal differentiation. Heterogeneity of satellite cells has also been discussed (58). Ten percent of quiescent satellite stem cells are $Pax7^+$ $Myf5^-$, whereas 90% of committed quiescent satellite cells are $Pax7^+$ $Myf5^+$ and are activated to subsequently coexpress MyoD, undergo limited proliferation, and then differentiate into $Pax7^-$ $MyoD^+$ cells (58, 59). We could not identify which Pax7-positive cells IBS008738 increased in the early phase after injury. We speculate the IBS008738 promotes both self-renewal of satellite stem cells and the commitment to $Pax7^+$ $Myf5^+$ satellite cells in response to injury and that it also promotes myogenic differentiation to $Pax7^+$ $Myf5^+$ $MyoD^+$ cells, which further differentiate to $Pax7^-$ $MyoD^+$ cells and at the same time harbor the subpopulation that returns to quiescent satellite cells. Thus, IBS008738 overall facilitates muscle repair with the replenishment of satellite cells. However, in order to understand how IBS008738 works, a more detailed analysis of the role of TAZ in satellite cells is necessary. IBS008738 also prevents dexamethasone-induced muscle atrophy. IBS008738 suppresses the expression of MuRF-1 and atrogin-1 and increases protein synthesis (Fig. 9). On the other hand, IBS008738 does not significantly induce EMT in the cancer cells tested (Fig. 10). These observations imply that IBS008738 may be useful for the treatment and prevention of muscle atrophy.

In this paper, we have introduced a novel cell-based assay to screen for TAZ activators. As compounds with various targets and a wide spectrum of cellular phenotypes are obtained with this assay, the collection works as a minilibrary of TAZ activators. Researchers can perform further selection based on the different cellular outputs as readouts and obtain compounds that function according to their interests.

ACKNOWLEDGMENTS

We are grateful for Hiroshi Asahara (Tokyo Medical and Dental University), Yasutomi Kamei (Kyoto Prefectural University), Hiroki Kurihara (The University of Tokyo), Yoshihiro Ogawa (Tokyo Medical and Dental University), Hiroshi Sasaki (Kumamoto University), Kenji Miyazawa (Yamanashi University), Kohei Miyazono (The University of Tokyo), Hiroshi Takayanagi (The University of Tokyo), and Sumiko Watanabe (The University of Tokyo) for materials and advice.

This work was supported by research grants from the Ministry of Education, Sports, Science, and Technology (17081008), the Japan Society for the Promotion of Science (22790275 and 22590267), the Suzuken Memorial Foundation, the Nakatomi Foundation, the Uehara Memorial Foundation, and the Naito Foundation. Z.Y. was supported by a Japanese Government (Monbukagakusho) (MEXT) scholarship.

REFERENCES

1. **Kanai F, Marignani PA, Sarbassova D, Yagi R, Hall RA, Donowitz M, Hisaminato A, Fujiwara T, Ito Y, Cantley LC, Yaffe MB.** 2000. TAZ: a novel transcriptional co-activator regulated by interactions with 14-3-3 and PDZ domain proteins. EMBO J. **19:**6778–6791. http://dx.doi.org/10.1093/emboj/19.24.6778.
2. **Hong W, Guan KL.** 2012. The YAP and TAZ transcription co-activators: key downstream effectors of the mammalian Hippo pathway. Semin. Cell Dev. Biol. **23:**785–793. http://dx.doi.org/10.1016/j.semcdb.2012.05.004.
3. **Wang K, Degerny C, Xu M, Yang XJ.** 2009. YAP, TAZ, and Yorkie: a conserved family of signal-responsive transcriptional coregulators in animal development and human disease. Biochem. Cell Biol. **87:**77–91. http://dx.doi.org/10.1139/O08-114.
4. **Sudol M.** 1994. Yes-associated protein (YAP65) is a proline-rich phosphoprotein that binds to the SH3 domain of the Yes proto-oncogene product. Oncogene **9:**2145–2152.
5. **Bao Y, Hata Y, Ikeda M, Withanage K.** 2011. Mammalian Hippo pathway: from development to cancer and beyond. J. Biochem. **149:**361–379. http://dx.doi.org/10.1093/jb/mvr021.
6. **Pan D.** 2010. The Hippo signaling pathway in development and cancer. Dev. Cell **19:**491–505. http://dx.doi.org/10.1016/j.devcel.2010.09.011.
7. **Oka T, Remue E, Meerschaert K, Vanloo B, Boucherie C, Gfeller D, Bader GD, Sidhu SS, Vandekerckhove J, Gettemans J, Sudol M.** 2010. Functional complexes between YAP2 and ZO-2 are PDZ domain-dependent, and regulate YAP2 nuclear localization and signalling. Biochem. J. **432:**461–472. http://dx.doi.org/10.1042/BJ20100870.
8. **Remue E, Meerschaert K, Oka T, Boucherie C, Vandekerckhove J, Sudol M, Gettemans J.** 2010. TAZ interacts with zonula occludens-1 and -2 proteins in a PDZ-1 dependent manner. FEBS Lett. **584:**4175–4180. http://dx.doi.org/10.1016/j.febslet.2010.09.020.
9. **Chan SW, Lim CJ, Chong YF, Pobbati AV, Huang C, Hong W.** 2011. Hippo pathway-independent restriction of TAZ and YAP by angiomotin. J. Biol. Chem. **286:**7018–7026. http://dx.doi.org/10.1074/jbc.C110.212621.
10. **Zhao B, Li L, Lu Q, Wang LH, Liu CY, Lei Q, Guan KL.** 2011. Angiomotin is a novel Hippo pathway component that inhibits YAP oncoprotein. Genes Dev. **25:**51–63. http://dx.doi.org/10.1101/gad.2000111.
11. **Dupont S, Morsut L, Aragona M, Enzo E, Giulitti S, Cordenonsi M, Zanconato F, Le Digabel J, Forcato M, Bicciato S, Elvassore N, Piccolo S.** 2011. Role of YAP/TAZ in mechanotransduction. Nature **474:**179–183. http://dx.doi.org/10.1038/nature10137.
12. **Halder G, Dupont S, Piccolo S.** 2012. Transduction of mechanical and cytoskeletal cues by YAP and TAZ. Nat. Rev. Mol. Cell Biol. **13:**591–600. http://dx.doi.org/10.1038/nrm3416.
13. **Wrighton KH.** 2011. Mechanotransduction: YAP and TAZ feel the force. Nat. Rev. Mol. Cell Biol. **12:**404. http://dx.doi.org/10.1038/nrm3145, http://dx.doi.org/10.1038/nrm3136.
14. **Azzolin L, Zanconato F, Bresolin S, Forcato M, Basso G, Bicciato S, Cordenonsi M, Piccolo S.** 2012. Role of TAZ as mediator of Wnt signaling. Cell **151:**1443–1456. http://dx.doi.org/10.1016/j.cell.2012.11.027.
15. **Imajo M, Miyatake K, Iimura A, Miyamoto A, Nishida E.** 2012. A molecular mechanism that links Hippo signalling to the inhibition of Wnt/β-catenin signalling. EMBO J. **31:**1109–1122. http://dx.doi.org/10.1038/emboj.2011.487.
16. **Varelas X, Miller BW, Sopko R, Song S, Gregorieff A, Fellouse FA, Sakuma R, Pawson T, Hunziker W, McNeill H, Wrana JL, Attisano L.** 2010. The Hippo pathway regulates Wnt/beta-catenin signaling. Dev. Cell **18:**579–591. http://dx.doi.org/10.1016/j.devcel.2010.03.007.
17. **de Cristofaro T, Di Palma T, Ferraro A, Corrado A, Lucci V, Franco R, Fusco A, Zannini M.** 2011. TAZ/WWTR1 is overexpressed in papillary thyroid carcinoma. Eur. J. Cancer **47:**926–933. http://dx.doi.org/10.1016/j.ejca.2010.11.008.
18. **Wang L, Shi S, Guo Z, Zhang X, Han S, Yang A, Wen W, Zhu Q.** 2013. Overexpression of YAP and TAZ is an independent predictor of prognosis in colorectal cancer and related to the proliferation and metastasis of colon cancer cells. PLoS One **8:**e65539. http://dx.doi.org/10.1371/journal.pone.0065539.
19. **Wei Z, Wang Y, Li Z, Yuan C, Zhang W, Wang D, Ye J, Jiang H, Wu Y, Cheng J.** 29 March 2013. Overexpression of Hippo pathway effector TAZ in tongue squamous cell carcinoma: correlation with clinicopathological features and patients' prognosis. J. Oral Pathol. Med. (Epub ahead of print.) http://dx.doi.org/10.1111/jop.12062.
20. **Yuen HF, McCrudden CM, Huang YH, Tham JM, Zhang X, Zeng Q, Zhang SD, Hong W.** 2013. TAZ expression as a prognostic indicator in colorectal cancer. PLoS One **8:**e54211. http://dx.doi.org/10.1371/journal.pone.0054211.
21. **Zhou Z, Hao Y, Liu N, Raptis L, Tsao MS, Yang X.** 2011. TAZ is a novel oncogene in non-small cell lung cancer. Oncogene **30:**2181–2186. http://dx.doi.org/10.1038/onc.2010.606.
22. **Bhat KP, Salazar KL, Balasubramaniyan V, Wani K, Heathcock L, Hollingsworth F, James JD, Gumin J, Diefes KL, Kim SH, Turski A, Azodi Y, Yang Y, Doucette T, Colman H, Sulman EP, Lang FF, Rao G, Copray S, Vaillant BD, Aldape KD.** 2011. The transcriptional coactivator TAZ regulates mesenchymal differentiation in malignant glioma. Genes Dev. **25:**2594–2609. http://dx.doi.org/10.1101/gad.176800.111.
23. **Chan SW, Lim CJ, Guo K, Ng CP, Lee I, Hunziker W, Zeng Q, Hong W.** 2008. A role for TAZ in migration, invasion, and tumorigenesis of breast cancer cells. Cancer Res. **68:**2592–2598. http://dx.doi.org/10.1158/0008-5472.CAN-07-2696.
24. **Cordenonsi M, Zanconato F, Azzolin L, Forcato M, Rosato A, Frasson C, Inui M, Montagner M, Parenti AR, Poletti A, Daidone MG, Dupont S, Basso G, Bicciato S, Piccolo S.** 2011. The Hippo transducer TAZ confers cancer stem cell-related traits on breast cancer cells. Cell **147:**759–772. http://dx.doi.org/10.1016/j.cell.2011.09.048.
25. **Hao J, Zhang Y, Jing D, Li Y, Li J, Zhao Z.** 2014. Role of Hippo signaling in cancer stem cells. J. Cell Physiol. **229:**266–270. http://dx.doi.org/10.1002/jcp.24455.
26. **Skinner M.** 2012. Cancer stem cells: TAZ takes centre stage. Nat. Rev. Cancer **12:**82–83. http://dx.doi.org/10.1038/nrc3210.
27. **Chan SW, Lim CJ, Huang C, Chong YF, Gunaratne HJ, Hogue KA, Blackstock WP, Harvey KF, Hong W.** 2011. WW domain-mediated interaction with Wbp2 is important for the oncogenic property of TAZ. Oncogene **30:**600–610. http://dx.doi.org/10.1038/onc.2010.438.
28. **Chan SW, Lim CJ, Loo LS, Chong YF, Huang C, Hong W.** 2009. TEADs mediate nuclear retention of TAZ to promote oncogenic transformation. J. Biol. Chem. **284:**14347–14358. http://dx.doi.org/10.1074/jbc.M901568200.
29. **Zhang H, Liu CY, Zha ZY, Zhao B, Yao J, Zhao S, Xiong Y, Lei QY, Guan KL.** 2009. TEAD transcription factors mediate the function of TAZ in cell growth and epithelial-mesenchymal transition. J. Biol. Chem. **284:**13355–13362. http://dx.doi.org/10.1074/jbc.M900843200.
30. **Park KS, Whitsett JA, Di Palma T, Hong JH, Yaffe MB, Zannini M.** 2004. TAZ interacts with TTF-1 and regulates expression of surfactant protein-C. J. Biol. Chem. **279:**17384–17390. http://dx.doi.org/10.1074/jbc.M312569200.
31. **Murakami M, Nakagawa M, Olson EN, Nakagawa O.** 2005. A WW domain protein TAZ is a critical coactivator for TBX5, a transcription factor implicated in Holt-Oram syndrome. Proc. Natl. Acad. Sci. U. S. A. **102:**18034–18039. http://dx.doi.org/10.1073/pnas.0509109102.
32. **Varelas X, Sakuma R, Samavarchi-Tehrani P, Peerani R, Rao BM,**

Dembowy J, Yaffe MB, Zandstra PW, Wrana JL. 2008. TAZ controls Smad nucleocytoplasmic shuttling and regulates human embryonic stem-cell self-renewal. Nat. Cell Biol. **10:**837–848. http://dx.doi.org/10.1038/ncb1748.

33. **Varelas X, Samavarchi-Tehrani P, Narimatsu M, Weiss A, Cockburn K, Larsen BG, Rossant J, Wrana JL.** 2010. The Crumbs complex couples cell density sensing to Hippo-dependent control of the TGF-β-SMAD pathway. Dev. Cell **19:**831–844. http://dx.doi.org/10.1016/j.devcel.2010.11.012.
34. **Hong JH, Hwang ES, McManus MT, Amsterdam A, Tian Y, Kalmukova R, Mueller E, Benjamin T, Spiegelman BM, Sharp PA, Hopkins N, Yaffe MB.** 2005. TAZ, a transcriptional modulator of mesenchymal stem cell differentiation. Science **309:**1074–1078. http://dx.doi.org/10.1126/science.1110955.
35. **Cui CB, Cooper LF, Yang X, Karsenty G, Aukhil I.** 2003. Transcriptional coactivation of bone-specific transcription factor Cbfa1 by TAZ. Mol. Cell. Biol. **23:**1004–1013. http://dx.doi.org/10.1128/MCB.23.3.1004-1013.2003.
36. **Jeong H, Bae S, An SY, Byun MR, Hwang JH, Yaffe MB, Hong JH, Hwang ES.** 2010. TAZ as a novel enhancer of MyoD-mediated myogenic differentiation. FASEB J. **24:**3310–3320. http://dx.doi.org/10.1096/fj.09-151324.
37. **Murakami M, Tominaga J, Makita R, Uchijima Y, Kurihara Y, Nakagawa O, Asano T, Kurihara H.** 2006. Transcriptional activity of Pax3 is co-activated by TAZ. Biochem. Biophys. Res. Commun. **339:**533–539. http://dx.doi.org/10.1016/j.bbrc.2005.10.214.
38. **Benhaddou A, Keime C, Ye T, Morlon A, Michel I, Jost B, Mengus G, Davidson I.** 2012. Transcription factor TEAD4 regulates expression of myogenin and the unfolded protein response genes during C2C12 cell differentiation. Cell Death Differ. **19:**220–231. http://dx.doi.org/10.1038/cdd.2011.87.
39. **Zhu X, Topouzis S, Liang LF, Stotish RL.** 2004. Myostatin signaling through Smad2, Smad3 and Smad4 is regulated by the inhibitory Smad7 by a negative feedback mechanism. Cytokine **26:**262–272. http://dx.doi.org/10.1016/j.cyto.2004.03.007.
40. **Judson RN, Gray SR, Walker C, Carroll AM, Itzstein C, Lionikas A, Zammit PS, De Bari C, Wackerhage H.** 2013. Constitutive expression of Yes-associated protein (Yap) in adult skeletal muscle fibres induces muscle atrophy and myopathy. PLoS One **8:**e59622. http://dx.doi.org/10.1371/journal.pone.0059622.
41. **Watt KI, Judson R, Medlow P, Reid K, Kurth TB, Burniston JG, Ratkevicius A, De Bari C, Wackerhage H.** 2010. Yap is a novel regulator of C2C12 myogenesis. Biochem. Biophys. Res. Commun. **393:**619–624. http://dx.doi.org/10.1016/j.bbrc.2010.02.034.
42. **Sayer AA, Robinson SM, Patel HP, Shavlakadze T, Cooper C, Grounds MD.** 2013. New horizons in the pathogenesis, diagnosis and management of sarcopenia. Age Ageing **42:**145–150. http://dx.doi.org/10.1093/ageing/afs191.
43. **Bao Y, Nakagawa K, Yang Z, Ikeda M, Withanage K, Ishigami-Yuasa M, Okuno Y, Hata S, Nishina H, Hata Y.** 2011. A cell-based assay to screen stimulators of the Hippo pathway reveals the inhibitory effect of dobutamine on the YAP-dependent gene transcription. J. Biochem. **150:**199–208. http://dx.doi.org/10.1093/jb/mvr063.
44. **Ikeda M, Kawata A, Nishikawa M, Tateishi Y, Yamaguchi M, Nakagawa K, Hirabayashi S, Bao Y, Hidaka S, Hirata Y, Hata Y.** 2009. Hippo pathway-dependent and -independent roles of RASSF6. Sci. Signal. **2:**ra59. http://dx.doi.org/10.1126/scisignal.2000300.
45. **Hirabayashi S, Nakagawa K, Sumita K, Hidaka S, Kawai T, Ikeda M, Kawata A, Ohno K, Hata Y.** 2008. Threonine 74 of MOB1 is a putative key phosphorylation site by MST2 to form the scaffold to activate nuclear Dbf2-related kinase 1. Oncogene **27:**4281–4292. http://dx.doi.org/10.1038/onc.2008.66.
46. **Bao Y, Sumita K, Kudo T, Withanage K, Nakagawa K, Ikeda M, Ohno K, Wang Y, Hata Y.** 2009. Roles of mammalian sterile 20-like kinase 2-dependent phosphorylations of Mps one binder 1B in the activation of nuclear Dbf2-related kinases. Genes Cells **14:**1369–1381. http://dx.doi.org/10.1111/j.1365-2443.2009.01354.x.
47. **Ota M, Sasaki H.** 2008. Mammalian Tead proteins regulate cell proliferation and contact inhibition as transcriptional mediators of Hippo signaling. Development **135:**4059–4069. http://dx.doi.org/10.1242/dev.027151.
48. **Kobayashi N, Goto K, Horiguchi K, Nagata M, Kawata M, Miyazawa K, Saitoh M, Miyazono K.** 2007. c-Ski activates MyoD in the nucleus of myoblastic cells through suppression of histone deacetylases. Genes Cells **12:**375–385. http://dx.doi.org/10.1111/j.1365-2443.2007.01052.x.
49. **Nelson JD, Denisenko O, Bomsztyk K.** 2006. Protocol for the fast chromatin immunoprecipitation (ChIP) method. Nat. Protoc. **1:**179–185. http://dx.doi.org/10.1038/nprot.2006.27.
50. **Goodman CA, Mabrey DM, Frey JW, Miu MH, Schmidt EK, Pierre P, Hornberger TA.** 2011. Novel insights into the regulation of skeletal muscle protein synthesis as revealed by a new nonradioactive in vivo technique. FASEB J. **25:**1028–1039. http://dx.doi.org/10.1096/fj.10-168799.
51. **Ikeda M, Hirabayashi S, Fujiwara N, Mori H, Kawata A, Iida J, Bao Y, Sato Y, Iida T, Sugimura H, Hata Y.** 2007. Ras-association domain family protein 6 induces apoptosis via both caspase-dependent and caspase-independent pathways. Exp. Cell Res. **313:**1484–1495. http://dx.doi.org/10.1016/j.yexcr.2007.02.013.
52. **Hong JH, Yaffe MB.** 2006. TAZ: a beta-catenin-like molecule that regulates mesenchymal stem cell differentiation. Cell Cycle **5:**176–179. http://dx.doi.org/10.4161/cc.5.2.2362.
53. **Lindon C, Montarras D, Pinset C.** 1998. Cell cycle-regulated expression of the muscle determination factor Myf5 in proliferating myoblasts. J. Cell Biol. **140:**111–118. http://dx.doi.org/10.1083/jcb.140.1.111.
54. **Schakman O, Kalista S, Barbé C, Loumaye A, Thissen JP.** 2013. Glucocorticoid-induced skeletal muscle atrophy. Int. J. Biochem. Cell Biol. **45:**2163–2172. http://dx.doi.org/10.1016/j.biocel.2013.05.036.
55. **Byun MR, Jeong H, Bae SJ, Kim AR, Hwang ES, Hong JH.** 2012. TAZ is required for the osteogenic and anti-adipogenic activities of kaempferol. Bone **50:**364–372. http://dx.doi.org/10.1016/j.bone.2011.10.035.
56. **Jang EJ, Jeong H, Kang JO, Kim NJ, Kim MS, Choi SH, Yoo SE, Hong JH, Bae MA, Hwang ES.** 2012. TM-25659 enhances osteogenic differentiation and suppresses adipogenic differentiation by modulating the transcriptional co-activator TAZ. Br. J. Pharmacol. **165:**1584–1594. http://dx.doi.org/10.1111/j.1476-5381.2011.01664.x.
57. **Olguín HC, Pisconti A.** 2012. Marking the tempo for myogenesis: Pax7 and the regulation of muscle stem cell fate decisions. J. Cell. Mol. Med. **16:**1013–1025. http://dx.doi.org/10.1111/j.1582-4934.2011.01348.x.
58. **Wang YX, Rudnicki MA.** 2012. Satellite cells, the engines of muscle repair. Nat. Rev. Mol. Cell Biol. **13:**127–133. http://dx.doi.org/10.1038/nrm3265.
59. **Zammit PS, Golding JP, Nagata Y, Hudon V, Partridge TA, Beauchamp JR.** 2004. Muscle satellite cells adopt divergent fates: a mechanism for self-renewal? J. Cell Biol. **166:**347–357. http://dx.doi.org/10.1083/jcb.200312007.